UNIVERSIDAD AUTÓNOMA DE NUEVO LEÓN
FACULTAD DE CIENCIAS QUÍMICAS

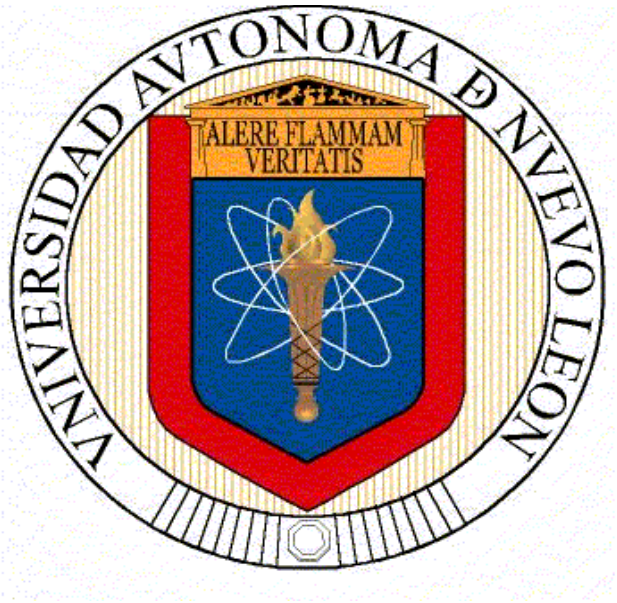

BROMATE AND CHROMATE REMOVAL FROM WATER BY DOUBLE LAYERED HYDROXIDES

POR

CECILIA PATRICIA VILLANUEVA RANGEL

COMO REQUISITO PARCIAL PARA OBTENER EL GRADO DE MAESTRÍA EN CIENCIAS CON ORIENTACIÓN EN PROCESOS SUSTENTABLES

SEPTIEMBRE, 2015

UNIVERSIDAD AUTONOMA DE NUEVO LEÓN
FACULTAD DE CIENCIAS QUÍMICAS

BROMATE AND CHROMATE REMOVAL FROM BY WATER DOUBLE LAYERED HYDROXIDES

POR

CECILIA PATRICIA VILLANUEVA RANGEL

COMO REQUISITO PARCIAL PARA OBTENER EL GRADO DE MAESTRÍA EN CIENCIAS CON ORIENTACIÓN EN PROCESOS SUSTENTABLES

SEPTIEMBRE, 2015

BROMATE AND CHROMATE REMOVAL FROM WATER BY DOUBLE-LAYERED HYDROXIDES

THESIS AUTHORIZATION:

Advisor: Dr. Refugio Bernardo García Reyes.

Co-Advisor: Dr. Juan Jacobo Ruiz Valdes.

Reviewer: Dr. Eduardo Soto Regalado.

Reviewer: Dra. María Teresa Garza González.

Reviewer: Dr. Felipe de Jesús Cerino Córdoba

CRÉDITOS

Esta tesis fue elaborada en la Escuela de Graduados en Ciencias de la Facultad de Ciencias Químicas de la Universidad Autónoma de Nuevo León, bajo la dirección del Dr. Refugio Bernardo García Reyes.

Durante la realización de la investigación el autor recibió una beca académica del Consejo Nacional de Ciencia y Tecnología (CONACYT) y de la Facultad de Ciencias Químicas de la Universidad Autónoma de Nuevo León.

El autor de esta tesis recibió recursos financieros por parte del Consejo Nacional de Ciencia y Tecnología para llevar a cabo una estancia de investigación en The University of Texas at Arlington en la división de Analytical Chemistry Research para concluir con la experimentación planteada en este trabajo.

DEDICATORIAS

Dedico este trabajo a Dios, que siempre me ha llevado de su mano y me ha dado todo lo que tengo; porque me ha regalado la vida, una familia extraordinaria, amigos para toda la vida y nunca me abandona.

A mi mamá, Patricia Rangel Muñiz, por todo el amor que me ha dado, que ha sido y seguirá siendo ejemplo y pilar en mi vida; por ser mi fortaleza, mi guía, mi amiga, por sufrir conmigo y también por las veces que ha sufrido en silencio para que yo no sufriera. Te quiero con todo el corazón.

A mis hermanos, José y Kary, que de cada uno tengo un pedacito; que de ellos he aprendido desde que nací y que son los mejores y más buenos hermanos que alguien pudiera tener y los quiero con todo mi corazón.

A mis sobrinas, Andrea y Sofía, que con sus sonrisas, abrazos o simplemente con su presencia me alegran hasta los días más difíciles y que aunque estén pequeñitas siempre encuentran la manera de hacerme sentir querida.

A mi papá, José Luis Villanueva Hinojosa, que aunque no lo tenga físicamente conmigo, no me olvido de él ni un solo día, y que en cada paso que doy lo recuerdo, y lo extraño.

A mis amigos fuera y dentro de la escuela: Gama, Fer, Gera, Christopher, Meli, Fanny, Aarón, Pablo, Jessica, Fabián, Jacinto y todos aquellos que aunque no estén nombrados aquí han ayudado a cumplir esta meta y además compartir momentos importantes en mi vida, los aprecio muchísimo.

AGRADECIMIENTOS

´

Le doy gracias a Dios, por poner en mi camino a tantas buenas personas, que con su amabilidad, tiempo e inteligencia me han dado la oportunidad de mejorar y también porque con cada cosa que existe me hace saber que siempre estará conmigo.

Al Dr. Refugio Bernardo García Reyes por darme la oportunidad de trabajar con él y su grupo de investigación, por sus enseñanzas, paciencia, sus consejos y por compartir con nosotros su tiempo, su casa y su amistad.

Al Dr. Juan Jacobo Ruiz Valdés, por todo su tiempo, consejos, su disponibilidad y ganas de escucharme y apoyarme siempre.

Al Dr. Purnendu Dasgupta, por la gran oportunidad que me permitió al trabajar con él y su grupo de trabajo tan acogedor, por todas las enseñanzas que compartió y su hospitalidad. Nunca olvidaré todo lo que viví al estar con ellos.

A la Dra. Teresa Garza González, por su gentileza, sus detalles, sus consejos y correcciones para mejorar este trabajo y por el tiempo que nos ha dado a todos.

Al Dr. Eduardo Soto Regalado que con sus correcciones, su tiempo, con su amabilidad y su interés este trabajo se ha enriquecido mucho.

A la Dra. Aracely Hernández Ramírez, por su comprensión, disposición, interés, y ayuda para este proyecto.

A Rocío Giselle Espinosa Silva, Alan Enrique Jasso Ríos, Roberto David Rentería Escamilla porque además de ayudar en la experimentación de esta tesis, compartimos muchos momentos juntos y siempre me dieron un apoyo que por el cuál siempre les estaré agradecida.

A Martín Garza que a pesar de la distancia, supo ayudarme siempre y me libró de dificultades.

Le agradezco a la University of Texas at Arlington por la infraestructura, equipos, reactivos facilitados para concluir las pruebas de esta tesis y a toda la gente que me dio su tiempo para compartirme sus enseñanzas, consejos y también escuchar todas mis dudas. Gracias a Brian, Philip, Akinde, Min, Chuchu, Hongzhu, Huang, Jacklyn, Mousavi y Nouroozi, por toda su paciencia, amabilidad, enseñanzas, consejos, y amistad, nunca los olvidaré.

Finalmente, le agradezco a la División de Posgrado de la Facultad de Ciencias Químicas por la infraestructura facilitada para la realización de esta investigación y a todos quien lo hacen posible.

EL AGRADECIMIENTO ES LA MEMORIA DEL CORAZÓN,
¡GRACIAS A TODOS!

TABLE OF CONTENTS

CRÉDITOS ii

DEDICATORIAS v

AGRADECIMIENTOS vi

LIST OF TABLES x

LIST OF FIGURES xi

ABSTRACT ..... **Error! Bookmark not defined.**

1. Introduction 1

1.1 Bromate in drinking water 1

1.2 Chromate in drinking water 2

1.3 Water treatment processes 2

1.3.1 Coagulation-flocculation 3

1.3.2 Ion exchange 3

1.3.3 Reverse osmosis 4

1.3.4 Adsorption processes 4

1.4 Adsorbents 9

1.4.1 Activated carbon 9

1.4.2 Zeolites 11

1.4.3 Polymer resins 12

1.4.4 Biosorbents 13

1.4.5 Clays 13

2 Background 19

2.1 Bromate removal methods 19

2.1.1 Bromate determination methods 20

2.2 Chromate removal methods 20

2.2.1 Chromate determination method 21

2.3 Double-layered hydroxides structure 21

2.4 Legal framework 22

3 Research motivation 23

4 Hypothesis 23

5 Objectives 23
5.1 General objective 23
5.2 Specific objectives 24
6 Methodology 24
6.1 Synthesis of Mg-Al Double-layered hydroxides with carbonate as the exchanging anion 24
6.2 Characterization of Mg-Al Double-layered hydroxides with carbonate as exchange anion 25
6.3 Synthesis and characterization of Mg-Al Double-layered hydroxides with chloride as the exchanging anion 26
6.4 Characterization of Mg-Al Double-layered hydroxides with chloride as exchanging anion 26
6.5 Calcination of Mg-Al Double-layered hydroxides 26
6.6 Characterization of calcined Mg-Al Double-layered hydroxides 26
6.7 Screening adsorption and desorption tests 26
6.8 Additional characterization 27
6.9 Chromate isotherms 27
6.10 Bromate isotherms 28
6.11 Chromate kinetic studies 28
6.12 Bromate kinetic studies 29
6.13 Packed bed column tests 29
6.14 Waste disposal 29
7 Results 30
7.1 Synthesis of Mg-Al Double-layered hydroxides 30
7.1.1 DLH with carbonate as exchanging anion 30
7.1.2 DLH with chloride as exchanging anion 31
7.2 Characterization of Mg-Al Double-layered hydroxides 32
7.2.1 X ray diffraction (XRD) 32
7.2.2 Thermogravimetric analysis ..... **Error! Bookmark not defined.**
7.3 Calcination of Mg-Al Double-layered hydroxides 36
7.4 Characterization of calcined Mg-Al Double-layered hydroxides 38
7.5 Screening adsorption and desorption tests 40
7.6 Additional characterization 42
7.6.1 Surface area analysis 42

7.6.2 Scanning electron microscopy 43
7.6.3 XRD after chromate adsorption 45
7.7 Chromate isotherms 46
7.8 Bromate isotherms 50
7.8 Chromate kinetic studies 53
7.9 Bromate kinetic studies 62
7.10 Packed bed column tests 63
8 General conclusions 67
9 References 68
Appendix A ..... **Error! Bookmark not defined.**

LIST OF TABLES

Table 1 Bromate and chromate maximum allowed level on drinking water by EPA, WHO and NOM. **23**

Table 2 Mass quantity per molar ratio of Mg: Al for 100 mL of water. **24**

Table 3 Phases present in each sample of Mg-Al double layered hydroxides by XRD. **32**

Table 4 Weight loss of DLH after calcination. **37**

Table 5 Phases present in each sample of Mg-Al double layered hydroxides by XRD. **38**

Table 6 Screening chromate adsorption tests. **41**

Table 7 Surface area values for the selected DLH. **44**

Table 8 Weight and atomic percent for the selected DLH after chromate adsorption. **45**

Table 9 Maximum adsorption capacities of chromate on the selected DLH adsorbents and CAGC at different pH values. **50**

Table 10 Maximum adsorption capacity of bromate on calcined DLH and activated carbon at different pH values. **51**

Table 11 Maximum adsorption capacity of bromate onto raw (CGAC) and modified activated carbon (MAC) at pH 6, 7 and 8. **52**

Table 12 Number, quantity, and time of the aliquots taken in kinetic studies. **53**

Table 13 Values of adsorption capacity (q_e) and C_e/C_o at 100, 200, and 300 rpm. **55**

Table 14 Values of adsorption capacity (q_e) and C_e/C_o for the oscillatory, magnetic, and intermittent mixing systems. **60**

Table 15 Adsorption kinetics profile for chromate in the intermittent and no air presence. **61**

Table 16 Adsorption kinetics for bromate in the intermittent and no-air intermittent-stirred. **63**

LIST OF FIGURES

Figure 1 Chromium speciation diagram. **2**

Figure 2 Schematic of an adsorbent particle depicting the surroundings stagnant fluid film. **7**

Figure 3 Sodium Zeolite A, an example of a common zeolite structure. **12**

Figure 4 Brucite sheet section showing Mg^{2+} centers coordinated with six hydroxyl anions and each hydroxyl anion with three Mg^{2+} cations; also two brucite sheets which thickness corresponds to basal space. **15**

Figure 5 Structure of Mg/Al double-layered hydroxides with carbonate as the exchanging anion. a) View from plane a, b) view from plane b, c) view from plane c and d) random view [2]. **22**

Figure 6 Kinetic studies mixing system. A) solution container (1 L beaker), b) vertical hollow shaft motor with 3 prop propeller of 3.5 cm each one, c) mixing speed controller (10-500 rpm) and d) 60 cm metallic motor holder. **29**

Figure 7 Mg-Al double-layered hydroxides with carbonate as exchanging anion with four different molar ratios. a) DLH1100 b) DLH21100 c) DLH31100 and d) DLH41100. **30**

Figure 8 Mg-Al double-layered hydroxides with chloride as exchange anion with best molar ratio (DLHCL31100). **31**

Figure 9 X-ray diffractograms of dried Mg-Al double layered hydroxides at different Mg/Al molar ratio (1 to 4) with carbonate and chloride as exchanging anions. **33**

Figure 10 Water and exchanging anions bonded to DLH sheets. **35**

Figure 11 Thermogravimetric analysis of DLH21100, DLH31100 and DLHCL31100. **36**

Figure 12 Mg-Al double-layered hydroxides at 400, 500 and 600 °C. a) DLH21400, b) DLH21500, c)DLH21600, d)DLH31400, e)DLH31500, f) DLH31600, g) DLHCL31400, h) DLHCL31500 and i) DLHCL31600 **37**

Figure 13 X-ray diffractograms of Mg-Al double layered hydroxides at different Mg/Al molar ratio (1 to 4) with carbonate and chloride as exchanging anions at 400, 500 and 600°C. **40**

Figure 14 SEM images for a) DLH31100 b) DLH31500 c) DLH31500 after chromate adsorption. **45**

Figure 15 XRD diffractogram for DLH31500 after chromate adsorption at pH 6. **46**

Figure 16 Chromate anion bonded to DLH sheets. **47**

Figure 17 Chromate adsorption isotherms for DLH31500 at pH 6, 7 and 8 and activated carbon at pH 6. **48**

Figure 18 Chromate adsorption isotherms for DLH31600 at pH 6, 7 and 8 and activated carbon at **48**

pH 6.

Figure 19 Chromate adsorption isotherms for DLHCL31500 at pH 6, 7 and 8 and activated carbon at pH 6. **49**

Figure 20 Chromate adsorption isotherms for DLHCL31600 at pH 6, 7 and 8 and activated carbon at pH 6. **49**

Figure 21 Bromate adsorption isotherms for selected double-layered hydroxides (DLH31500) at pH 6, 7 and 8 and activated carbon (CGAC) at pH 6. **51**

Figure 22 Modified activated carbon adsorption isotherms at pH 6, 7 and 8 for bromate removal. **52**

Figure 23 Adsorption kinetics of chromate onto DLH31500 at pH 6 at 100 rpm. **54**

Figure 24 Adsorption kinetics of chromate onto DLH31500 at pH 6 at 200 rpm. **54**

Figure 25 Adsorption kinetics of chromate onto DLH31500 at pH 6 at 300 rpm. **55**

Figure 26 XRD diffractogram for DLH31500 at 100 and 400 rpm. **57**

Figure 27 Adsorption kinetics of chromate on DLH31500 with magnetic-stirred system. **58**

Figure 28 Adsorption kinetics of chromate on DLH31500 with oscillatory-stirred system. **59**

Figure 29 Adsorption kinetics of chromate on DLH31500 with intermittent-stirred system. **59**

Figure 30 Adsorption kinetics of chromate on DLH31500 for no-air intermittent-stirred system. **61**

Figure 31 Bromate adsorption kinetics for DLH31500 for no-air intermittent-stirred system. **62**

Figure 32 Packed bed column tests for chromate adsorption. **64**

Figure 33 Packed bed column tests for bromate adsorption. **65**

Figure 34 Packed bed column with DLH31500. A) Packed bed column (5 mL pipette tip), b) peristaltic pump (0.3 µL/min to 30 mL/min), c) 1 Liter plastic initial solution container, d) 60 cm metallic column holder, and e) 50 mL plastic final concentration container. **66**

ABSTRACT

CECILIA PATRICIA VILLANUEVA RANGEL

Graduation Date: September, 2015

Universidad Autónoma de Nuevo León

Facultad de Ciencias Químicas

Thesis title: BROMATE AND CHROMATE REMOVAL FROM WATER BY DOUBLE-LAYERED HYDROXIDES

Number of pages: 73

Candidate for the Master Degree in Sciences with Orientation in Sustainable Processes

Study area: Sustainable Processes.

Purpose and method of study: To remove bromate and chromate from water, common methods include ion exchange, coagulation-flocculation processes, reduction-precipitation, etc., but these strategies can present some important disadvantages like incomplete removal, high cost, continuous use of reagents, and high energy costs. One of the most promising removal methods is the adsorption processes because of its high efficiency and low cost. In this study, double-layered hydroxides (DLH) of aluminum and magnesium were synthesized at different Mg/Al molar ratios with Cl^- and CO_3^{-2} as the exchanging anions in order to remove bromate and chromate from water by adsorption processes. The synthesized materials were calcined at 400, 500, and 600°C to evaluate the effect of this treatment on the adsorption of the target pollutants.

Contribution and Conclusions: Among all the tested adsorbents, DLH with a Mg/Al molar ratio of 3:1, with carbonate as the exchange anion, and calcined at 500 °C (identified as DLH31500) presented a maximum adsorption capacity for chromate and bromate of 248.9 and 134.1 mg/g at pH 6, respectively. In contrast, adsorption capacity onto granular activated carbon achieved 35.76 and 69.1 mg/g for chromate and bromate, respectively, which is seven times and two fold lower than DLH31500. When the activated carbon was modified with ammonia, bromate adsorption capacity decreased 12% in comparison with the raw activated carbon. Adsorption kinetics of chromate on DHL31500 was affected by the stirring type (mechanical, magnetic, intermittent, and oscillatory mixing), but the intermittent mode allowed the maximum chromate uptake as well as bubbling argon gas to the initial solution in order to displace the air in a closed vessel and to avoid carbon dioxide absorption along the experiment. The adsorption equilibrium was reached at 2880 min and the chromate adsorption capacity was 169.38 mg/g. In the same system, bromate adsorption equilibrium was reached at 5760 min, and the adsorption capacity was 110.38 mg/g. For continuous adsorption tests, a packed bed column with DLH31500 was built and chromate (20 mg/L) and bromate (5 mg/L) solutions were fed to the column. Chromate and bromate adsorption capacities of 104.66 and 45.77 mg/g were achieved, which successfully treated 7.85 and 13.73 L, respectively. Finally, it was verified by X-Ray diffraction that DLH is mainly formed of layers,

but after thermal treatment this structure is disassembled. Nevertheless, DLH layers reassemble after chromate adsorption, forming again the characteristic layers of a DLH (*i.e.* a memory effect). In conclusion, DLH is a promising adsorbent for the removal of bromate and chromate pollutants from aqueous solutions.

ADVISOR SIGNATURE: _____

Dr. Refugio Bernardo García Reyes

1. Introduction

Water is one of the most used resources on earth for humans and living beings. Because of its high demand, this natural resource had been seriously affected by pollution since long time ago, when the wastewater of industries or home activities, were irresponsibly disposed of into potential drinking water sources such as rivers, lakes, seas and oceans [1]. Once ecology and environmental education started, wastewaters began to be used into irrigation processes and drains. Nowadays with the population growth, it is necessary to treat polluted waters to use them in high quality processes and also to offer safe drinking water to reduce the impact on population's health [2]. Water and wastewater management must assure the collection, the treatment and the correct distribution of both drinking water and wastewater to guarantee the health and welfare of society [3].

1.1 Bromate in drinking water

There are some traditional methods to clean and disinfect drinking water, like chloration, but studies proved that the disinfection method can produce trihalomethanes and haloacetic acids [4]. An alternative method for chloration is the ozonation [5], which is one of the most promising disinfection methods for water.

Even though ozonation is an effective disinfection method, it can produce byproducts highly toxic like bromate [6]. Bromate ions are not commonly found in drinking water, but if water contains bromide ions (from exchange ion resins used in water softening, or by seawater intrusion in aquifers) while ozonation process is running, bromide ions are oxidized to bromate.

Studies of bromate removal have been of great relevance in health area around the world because bromate had been considered in Group 2B or "Possible human carcinogen" for the IARC (International Agency for Research on Cancer) [7]. Available information shows some of the consequences of bromate poisoning, one of the most serious is the growth of cancerous tumors in liver, kidneys and thyroids, also can cause nervous system weakness, kidney failure, and severe gastrointestinal irritation [8].Some other toxic effects of bromate salt ($NaBrO_3$ and $KBrO_3$) when ingested are: nausea, vomit, abdominal pain, diarrhea, anury, anemia, pulmonary edema, deafness, etc. [9]. Besides, consumption of products that may contain bromate is not yet regulated, and with this there is an increase in the risk on health complications.

1.2 Chromate in drinking water

Several metals (like chromium, among others) are toxic and can cause several damages to humans and other species' metabolisms. The removal of these metals has a great impact due to their toxicity, persistence in nature, bio-accumulation tendency, etc. In the case of chromium (Figure 1) can be found in water by industrial effluents from different processes as: tannery, metal finishing, textile industry, metal plating, and some others [10]. According to the pH and concentration and forms of chromium can vary. Cr (IV) can form several species, namely Cr (IV) is found as CrO_4^{2-}, $HCrO_4^-$ or $Cr_2O_7^{2-}$, depending on both pH and total Cr (IV) concentration as is shown in Figure 1.

Experimental studies in chromium removal had had huge impact in both scientific and health areas because chromium had been reported as a possible carcinogen, causing problems with human immune system [11]. Also, the exposure to hexavalent chromium causes liver and kidney damage, internal hemorrhage, nausea, diarrhea, dermatitis, internal hemorrhage, and respiratory problems [9, 11, 12].

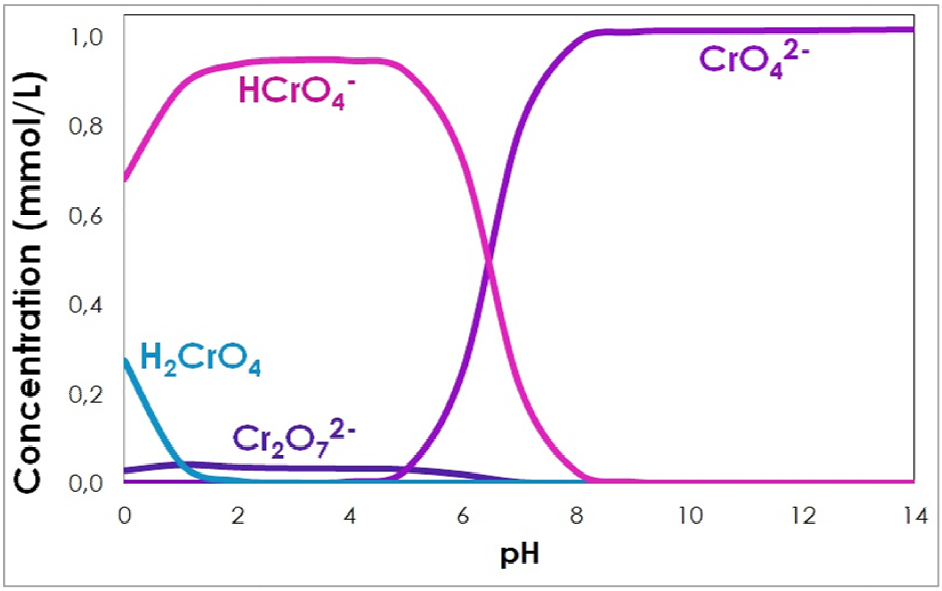

Figure 1 Chromium speciation diagram.

1.3 Water treatment processes

A number of methods have been developed to remove several pollutants from aqueous solutions such as heavy metals, natural organic matter, solvents, dyes, bromate and chromate oxyanions, etc. For metal-containing wastewater, researchers have tried processes such as reduction-precipitation, coagulation-flocculation, ion exchange, reduction by UV radiation, reverse osmosis, and adsorption [12]. The most common methods used to reduce the quantity of bromate and

chromate species in water are coagulation-flocculation [13, 14], ion exchange [15, 16], reverse osmosis [17], and adsorption process [7, 10, 18, 19]. In the following section, these methods are discussed more in detail.

1.3.1 Coagulation-flocculation

Water can contain particles that can be separated by gravity or dispersed particles that do not easily sediment (commonly known as colloids). Colloids are particles that are stabilized in water by a series of charges of the same sign in all the surface, making that if one particle is close to another one they will repel each other; so, this will avoid the collision of particles and no coagulates can be formed and no precipitation will exist. The coagulation-flocculation processes destabilize the colloids and sedimentation can be reached by adding chemicals and mixing.

The first step is the coagulation which is the destabilization of colloid particles produced by the elimination of electrical layers around them by the coagulant addition (aluminum or iron sulfate or chloride salts). The second step is the flocculation process (enhanced by an organic polymer as the flocculant) where an agglomeration of destabilized particles is carried out first as microflocs and then as more voluminous flocs, which being heavier can sediment and be separated from the aqueous solutions in a clarifier and/or by filtration.

1.3.2 Ion exchange

This is a process of exchange of ions between two electrolytes or between an electrolyte solution and a complex. Most of the times this term is used to designate a purification process, separation, or refinement of ion-containing solutions with solid polymeric or mineral ion exchangers. Some of the most typical ion exchangers are ion exchange resins, zeolites, clays, and some others.

Ion exchangers are either cation exchangers that exchange positively charged ions or anion exchangers that exchange negatively charged ions. Amphoteric exchangers are able to exchange both cations and anions simultaneously, but this can be more efficient in mixed beds that contain a mixture of anion and cation exchange resins.

Ion exchange materials can be unselective or have preferences for certain ions, depending on their chemical structure. This can be dependent on the size of the ions, charge, or their structure.

Ion exchange is a reversible process and the ion exchanger can be regenerated or loaded with desirable ions by washing it with an excess of these ions.

1.3.3 Reverse osmosis

Reverse osmosis is a water purification process where a semipermeable membrane is used. In reverse osmosis, an applied pressure is used to break the osmotic pressure, a colligative property that is driven by chemical potential.

This process can be used to remove many types of molecules and ions from solutions and, for this reason it is used in both industrial effluents and drinking water treatment. The result is that the solute is retained on the pressurized side of the membrane and the pure solvent is allowed to pass to the other side. Selectivity is reached by a membrane that does not allow large molecules or ions through the pores, but should allow smaller components of the solution to pass easily.

1.3.4 Adsorption processes

The adsorption process is a mass transfer operation in which a selective removal of species of interest (adsorbate) exists and it can be present in gas or aqueous fluid over a solid surface (adsorbent) having a high affinity for the specie of interest [20].

Adsorption can be classified in two kinds: physical or chemical adsorption, depending on the force nature between adsorbates and adsorbent. Physical adsorption implies relatively weak forces; it is a rapid process caused by non-specific mechanisms such as binding by van der Waals forces and, therefore, it is reversible. Thus, desorption of the adsorbed solute can occur. The physical adsorption occurs at low temperatures and it is not site-specific. It is the most common mechanism for adsorbates removal in water treatment [21].

In chemical adsorption, a chemical bond is formed in the adsorption process, and usually occurs at high temperatures, as long as it form chemical bonds, it is irreversible and also it is site-specific.

Adsorption is a promisor removal process highly efficient with low costs of invests in energy and capital and the possibility of reuse adsorbents in multiple adsorption cycles, also this process do not generated sludge or a constant use of reagents.

1.3.4.1 Physical adsorption factors

The affecting factors to the physical adsorption are temperature, nature of the solvent, surface area of adsorbent, pore structure, solution pH, competition with other species, etc. [21].

Most of the times, an increment of temperature decreases the adsorption because molecules have the enough vibrational energy to desorb from the surface. Similarly, the solvent has an

important effect since it competes with the surface in attracting the solute that wants to be removed.

Likewise, the surface area is very important to the physical adsorption as it is the possible place where adsorption can occur, but it is necessary always to consider the size of the solute molecules. Furthermore, the pore structure is important because of pore diameters, which range can be less than 10 to 100,000 Å which size of molecules can pass in them [22].

The pH effect is extremely important when the adsorbing species are capable of ionizing in response to the pH. It is well known that substances are poorly absorbed when they are ionized. When pH is such that an adsorbable compound exists in ionized form, adjacent molecules of the adsorbed species on the adsorbent surface will repel each other, because they carry the same electrical charge, so the adsorbing species cannot pack together very densely on the adsorbent surface and the adsorbate uptake is low. When the adsorbing species are not ionized, no electrical repulsion exists, and the packing density on the adsorbent surface can be higher [23].On the other hand, under acidic conditions, the surface of adsorbent becomes highly protonated and favors the adsorption of anions and with the increased in the pH the degree of protonation of the surface reduces gradually and adsorption is decreased [24]. Furthermore, as pH increases there is competition between OH- and the anions in the aqueous solution. The net positive surface potential of sorbent decreases, resulting in the weakening of electrostatic forces between sorbent and sorbate, which ultimately leads to reduced sorption capacity [25].

Adsorbents have specific surface area which means that the presence of other adsorbates will imply competition for available adsorption sites, but as long as some adsorption sites can absorb only certain solutes, not all solutes compete for the same sites [21], but to know how much of an adsorbate can be adsorb by a adsorbent material, batch tests have to be perform so a maximum adsorption capacity (for a specific adsorbate) can be calculated.

1.3.4.2 Batch adsorption tests

Having a quantity of adsorbent in contact with a given volume of a liquid containing an adsorbable solute, adsorption will occur until equilibrium is achieved. The equilibrium state has certain solute concentration in the adsorbent (q_e) and a final solute concentration in the liquid phase (C_e).

There are two different batch adsorption methods, in the first one, the adsorbent mass is fixed and the initial adsorbate concentration is varied in each experiment. In the second method, the initial adsorbate concentration is fixed and the quantity of adsorbent added to each batch experiment is varied.

No matter which technique is used, the mass of adsorbent as well as the initial and final adsorbate concentrations (C_o and C_e, respectively) has to be recorded to calculate the adsorption capacity.

The amount of solute adsorbed per unit mass of adsorbent (adsorption capacity as mg/g, mmol/g, etc.) is obtained by using the next mass balance expression:

$$Q_e = \frac{V(C_o - C_e)}{m} \qquad (1)$$

Any consistent unit set can be used for the quantities in this mass balance, one set might be: Q_e is the adsorption capacity (mg/g), C_o and C_e are the initial and equilibrium concentrations (mg/L) respectively; V is the solution volume (L) and m the dry mass of adsorbent (g).

Temperature (T) and pH conditions have to be specified to make comparisons of adsorption capacities among several combinations of conditions.

With the adsorption capacity calculated, isotherm as Langmuir and Freundlich models could be used to adjust the experimental data.

1.3.4.3 Isotherms models

An adsorption isotherm equation is an expression of the relation between the amount of solute adsorbed and the concentration of the solute in the fluid phase, at a specific pH and temperature.

When a solution is contacted with an adsorbent and the system is allowed to attain equilibrium, the rate at which molecules are absorbing to the surface is equal to the rate at which molecules are leaving the surface.

1.3.4.3.1 Langmuir isotherm

Langmuir adsorption isotherm implies the adsorbent surface as homogeneous, assumes also that all the adsorption sites have equal adsorbate affinity, adsorption allows accumulation only up to a monolayer and adsorption at one site does not affect adsorption at adjacent sites. The Langmuir isotherm can be represented by the following expression:

$$Q_e = \frac{Q_{max} b C_e}{1 + b C_e} \qquad (2)$$

Where Q_e is the adsorption capacity (mg/g), Q_{max} is the maximum adsorption capacity (mg/g), b is the relative energy of adsorption (L/mg), and C_e is the equilibrium concentration (mg/L).

1.3.4.3.2 Freundlich isotherm

The Freundlich adsorption isotherm describes the equilibrium on heterogeneous surface and does not assume monolayer capacity, and it is represented as:

$$Q_e = kC_e^{1/n} \qquad (3)$$

Where Q_e is the adsorbate quantity adsorbed per unit mass of adsorbent, k and n are Freundlich constants related to the adsorption capacity and adsorption intensity, respectively, and C_e is the equilibrium concentration (mg/L).

The Freundlich model does not impose any requirement that the coverage must approach a constant value corresponding to one complete monolayer as C_e gets higher. Indeed, the equation form shows that Q_e can continue to increase without bound as C_e increases, which means that Freundlich equation should fail at high C_e values; however, most real systems do not have high pollutants concentration in the adsorption step, so the values when Freundlich fail are not found.

1.3.4.4 Kinetic studies

Figure 2 shows a theoretical particle of adsorbent, visualized as spherical shape, with a smooth surface, even though, real adsorbent do not present perfect spherical forms. It is assume that the particle is initially solute-free, and that at zero time it is tossed into a relatively large volume of well-mixed liquid having an initial solute concentration C_o.

As shown in Figure 2, the adsorbent particle can be set with an immobile film of the liquid phase with a specific thickness. The transfer of solute through the liquid film surrounding the particle can be by molecular diffusion. If the thickness of the liquid film wants to be reduced, to decrease the external mass transfer resistance, the intensity of mixing has to be increased.

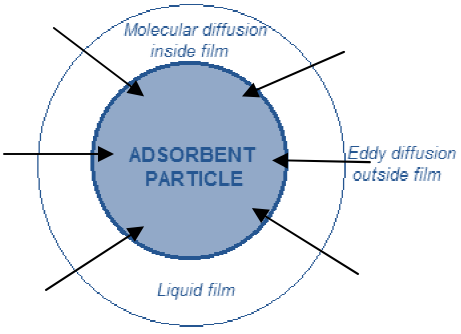

Figure 2 Schematic of an adsorbent particle depicting the surroundings stagnant fluid film.

Being a complex situation by all the zones which coexist in an adsorbent particle when it is in a liquid solution, the situation is simplify by establish only two zones; first, a stagnant region of a specific thickness in which all of the mass transfer resistance lies and, second, a homogenous region outside of that, in which no mass transfer resistance exists.

When the adsorption process starts, eventually a solute molecule reaches the pore at the surface and then it will diffuse through the liquid which pass in a tortuous network made of interconnected pores until each molecule finds a site to be adsorbed. The process to cover all the possible surface sites in a particle is a slow one.

So, there are two major resistances to mass transfer: the external resistance in the liquid phase and the internal resistance in the solid phase. Mass transfer through the surrounding film is modeled with the linear driving force (LDF):

$$\frac{\partial \bar{q}}{\partial t} = k_f S_o (C - C_i) \qquad (4)$$

Where $\bar{q}$ is the average solute concentration in the solid, C is the uniform concentration of solute in the liquid bulk far from the surface, C_i is the solute concentration in the liquid at the particle/liquid interface, S_o is the surface area of adsorbent particle per unit volume of the adsorbent particle and k_f is the film mass transfer coefficient.

The model for the solid phase is the homogeneous solid diffusion model (HSDM) which models mass transfer in the solid as diffusion in an amorphous and homogenous spherical particle.

HSDM model considers a mass transport mechanism across the hydrodynamic boundary layer surrounding the particle (adsorbent) and also an intraparticle resistance inside the adsorbent (surface diffusion).

$$\rho_p \frac{\partial q}{\partial t} = \frac{1}{r^2}\frac{\partial}{\partial r}\left[r^2 \left(D_S \frac{\partial q}{\partial r}\right)\right] \qquad (5)$$

The term on the left represents the accumulation of the adsorbate in the pore surface. On right the surface diffusion is represented. The initial and boundary conditions for equation 5 are:

$$t = 0 \quad 0 \le r \le R \quad q = 0$$

$$t > 0 \quad r = 0 \quad \frac{\partial q}{\partial r} = 0$$

$$t < 0 \quad r = 0 \quad \rho_p D_S \left(\frac{\partial q}{\partial r}\right)\Big|_{r=R} = k_L (C - C_S)$$

This equation considers that the liquid-phase surrounding the adsorbent particle is uniform and the equilibrium between liquid and solid phase is assumed to occur at the surface of the particle and the values of k_L and D_S can be determined by best fit correlation of the dynamic model with the experimental data [26].

1.3.4.5 Packed bed columns

Chemical engineering operations commonly use packed beds. These are devices in which a large surface area of contact between a liquid and a gas, or a solid and a gas or liquid is obtained to achieve rapid mass transfer and chemical reactions.

Packed bed column is a cylindrical column packed with certain packing material. The packing can be randomly filled with small objects like Rasching rings or material that can be a specifically designed structured packing. Several chemical engineering unit operations such as absorption, adsorption, distillation and extraction are carried out in packed bed columns. These packing materials develop a higher surface area available for transfer operations. Packed columns are also used for heterogeneous catalytic reactions [27].

In adsorption processes, packed bed columns are used to treat water in continuous mode. For screening tests, the packed bed column volume and a flow rate have to be fixed, and the pH has to be specified for results comparisons. To select the best values of column volume and flow rate, the empty bed contact time (EBCT) established an optimal working range (1-20 min) to assure the best column use. The EBCT is a measure of the time during which a water to be treated is in contact with the treatment medium in a contact vessel, assuming that all liquid passes through the empty vessel at the same velocity [20].

1.4 Adsorbents

An adsorbent is a solid material with the capacity of holding a substance on its surface and pores from gaseous or aqueous phases, and it is characterized by a high specific surface [28].

Adsorbents are commonly used in water treatment to remove pollutants; the most common adsorbents include activated carbon, zeolites, polymeric resins, and biosorbents, among others. Adsorbents can be synthesized or modified to be used in water and wastewater treatment in batch or continuous systems for the removal of pollutants at trace concentrations. In the following sections, a number of adsorbents are discussed in detail.

1.4.1 Activated carbon

Activated carbons are one of the most studied adsorbents. They are made from a wide variety of carbonaceous materials like coals, wood, peat, straws, shells, etc. With the chemical or physical activation and thermal treatment, precursors develop a large network of pores and high surface area such as 500 to 1500 m^2/g [29], and in this extensive surface area is where adsorption can occur.

The use of activated carbon in water treatment can involve either granular or powdered carbon. If the activated carbon is used in granular form, it is placed inside a vessel with screens in top and bottom to confine the material as a packed bed. If the carbon is used in powdered form, it is added to a stirred tank in which the water to be treat is contained.

As above-mentioned, activated carbons can be produced with most of the carbonaceous materials, but the activated carbon properties will vary with the precursor material [30]. Once that the starting material is chosen, a process to make the material to an activated carbon has to be selected. However, most of the processes consist of the pyrolysis followed by a stage of controlled oxidation to activate the carbon [29].

After the carbonation and activation processes, each material will develop specific physical properties. Activated carbons can contain inorganic constituents derived from the source material or added chemicals during manufacture. Some of the most important properties that have to be specified are: ash content, moisture, density, particle size, hardness, pore-size distribution, surface area, etc. [20, 30]

1.4.1.1 Physical properties

The ash content consists of the residue remaining when a sample of carbon is heated in an oxidizing atmosphere at 950 °C for about three hours. Ash contents range typically from 3 to 10 % of the original carbon weight. The ash extraction can be done by an acid washing step [31].

The density can be divided into three different densities: bulk density, particle density and real density. Bulk density is the weight per unit volume of a dry carbon in a packed bed, particle density is the density of a single particle, and the real density is that of the solid carbonaceous material alone after a displacement with helium is done.

The pore-size distribution represents the total volume of the pores in carbon particles per unit of weight of the carbon. The pore-size distribution depends on the precursor materials and also the activation methods. Pores are often classified as macropores (greater than 500 Å in diameter), micropores (less than 20 Å), and mesopores (between 20-500 Å) [32].

Surface area is calculated by the BET equation, the equation describes the formation of multilayers of condensed gas which occurs when an adsorbable gas such as nitrogen is contacted with the porous solid.

1.4.1.2 Standard adsorption tests

Some of the adsorption tests used to characterize the activated carbon, based on its ability to adsorb different kinds of molecules, are: iodine number, molasses number, methylene blue number, and carbon tetrachloride activity [29].

The iodine number is the amount of iodine adsorbed by activated carbon in equilibrium with a solution of I_2-KI and it indicates the surface area which exists in pore diameters greater than 10 Å.

The molasses number is a degree of decolorization of a standard molasses solution that has been diluted and standardized against standardized activated carbon. Due to the size of color bodies, the molasses number represents the potential pore volume available for larger adsorbing species.

Methylene blue number shows the adsorption capacity of activated carbon to adsorb molecules of that size and it is presented as the milligrams of methylene blue adsorbed by one gram of activated carbon.

The carbon tetrachloride activity is a good indicator of the total pore volume, because carbon tetrachloride (CCl_4) is a small molecule that can enter in very small pores.

1.4.2 Zeolites

Zeolites are microporous aluminosilicate minerals with well-defined structures commonly used as adsorbents. Their adsorbing properties were found out when the material was being heated and large amounts of steam were generated from all the adsorbed water. Generally they contain silicon, aluminum and oxygen in their framework and cations, water and/or other molecules within their pores. Many occur naturally as minerals, and are extensively mined in many parts of the world. Other kinds of zeolites are synthetic and are made commercially for specific uses, or produced by research scientists.

Because of their unique porous properties, zeolites are used in a variety of applications with a global market of several million tons per year. Zeolites are widely used as ion exchange beds in water treatment, softening, and other applications [33]. Furthermore, zeolites have the potential of providing precise and specific separation of gases including the removal of H_2O, CO_2 and SO_2 from natural gas streams. Other separations include noble gases, N_2, O_2, Freon and formaldehyde [34].

Synthetic zeolites are widely used as catalysts in the petrochemical industry in fluid catalytic cracking processes [35]. Zeolites confine molecules in small spaces, which cause changes in their structure and reactive activity. The specific activation modality of most zeolite catalysts used in petrochemical applications involves quantum-chemical Lewis acid site reactions, among other uses [33].

Zeolites have a porous structure that can hold a wide variety of cations, such as Na^+, K^+, Ca^{2+}, Mg^{2+} and others. These cations are held with really low forces and can readily be exchanged for others

in a contact solution. Some of the more common mineral zeolites are analcime, chabazite, clinoptilolite, heulandite, natrolite, phillipsite, and stilbite [36].

Also, zeolites are the aluminosilicate members of the family of molecular sieves, which refers to a particular property of selection molecules based on a size exclusion process. This is because of their regular pore structure, as can be seen in Figure 3. The maximum size of the molecular or ionic species that can enter the pores of a zeolite is controlled by the dimensions of the channels. These are conventionally defined by the ring size of the aperture.

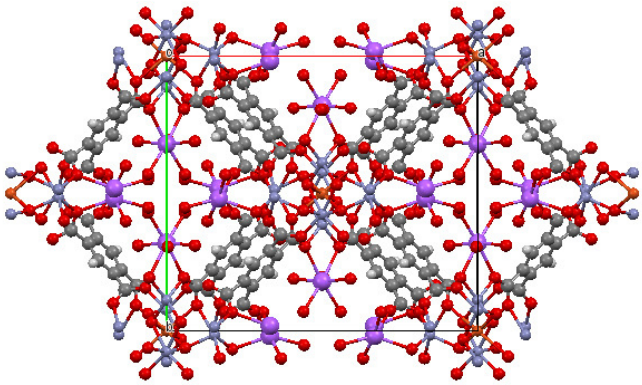

Figure 3 Sodium Zeolite A, an example of a common zeolite structure [37].

1.4.3 Polymer resins

Macroporous polymers are based on synthetic polymers joined with divinylbenzene, phenol-formaldehyde or acrylic ester. The union delivers high surface area as well as the firmness and mechanical strength [38].

The polymeric matrices can be functionalized with a variety of functional groups which give cation or anion exchange properties to the resins [39]. For example, polystyrene can be sulfonated with sulfuric acid resulting in a $-SO_3-H^+$ group attached to the benzene ring, and the proton can be easily exchanged with other cations. Likewise, attaching nitrogenous groups result in anion exchange resins, etc. [40].

Ion exchange resins are used for water treatment. Ionized pollutants are exchanged with ions that neutralize the charge of functional groups in the resins. The ion exchange resins which present higher ion exchange capacities are those based on weak bases and weak acids; but, renewal of strong-acid or strong-base resins is easier than for the weak-acid or weak-base resins. This could be related to the formation of covalent coordinated bonds between the pollutants and the functionalities of each resin [15].

1.4.4 Biosorbents

Biosorbents are materials with the capacity to remove organic or inorganic substances from aqueous solutions. Biosorbents are made of biological materials like living or dead biomasses [41].

Biosorption is used to describe a system where an adsorbate interacts with a biosorbent resulting in an accumulation at the solute-biosorbent interface, and then a reduction in the adsorbate concentration in solution is reached. Now-a-days, many biosorbents are investigated to remove pollutants from aqueous solutions, like seaweed, living or dead microorganism biomass, lignocellulosic materials, etc. [41, 42].

1.4.5 Clays

It is one of the oldest building materials on earth, among other ancient, naturally-occurring geologic materials such as stone and organic materials like wood. Between one-half and two-thirds of the world's population, in traditional societies as well as developed countries, still live or work in a building made with clay as an essential part of its load-bearing structure. Also a primary ingredient in many natural building techniques, clay is used to create adobe, cob, cordwood, etc., structures and building elements such as daub, clay plaster, clay render case, clay floors and clay paints [43].

Clays, from the geological point of view, are inorganic minerals with particle size equal or less than 2 μm. Chemical compositions can be varied, but most common ones are aluminosilicates which are characterized by crystalline laminar morphology. The sheets can be staggered forming a new type of structure which presents strong chemical bonds in two of their dimensions (crystallographic axis “a” and “b”) but they have weak interactions and their third dimension (crystallographic axis “c”) [44]. This results into molecules with unique physical and chemical properties like the capacity to adsorb ions in the interface.

A way to classify the laminar clays is with their function as ion adsorbent and related to this, the net charge that metallic sheets have. There are some clays (neutral clays) that do not present ability to adsorb ions [45]. If the net charge of the sheet is negative, in the interface will be cations equilibrating the charges (cationic clays), likewise, the sheets with positive charges will hold anions balancing the charges of the clay (anionic clays).

Anion clays have a crystalline hexagonal or octahedral structure. They have sheets of metallic cations positively charge, where the surface of sheet is occupied by hydroxyl groups, anions and water molecules [1].

Hidrotalcite is the most representative anion clay. It is a natural clay resulting of the isomorphic variations of brucite sheets [$Mg(OH)_2$] when Mg^{2+} cations are substituted with Al^{3+} cations and with this substitutions the net charge of the sheets turns positive.

In hidrotalcites, the predominant anion is carbonate. Double layered hydroxides are synthetic compounds with analogous structures to hidrotalcite. In literature, double-layered hydroxides are known as hidrotalcite-like compounds, anionic clays or synthetic clays [46].

1.4.5.1 Double-layered hydroxides

Double-layered hydroxides (DLH) are synthetic structures comprising hydroxylated layers with positive electrostatic charges stabilized by interlayer anions. The anion exchange capacity can be tuned during the synthesis unlike natural anion exchangers like clays. The hydroxyl groups that cover the surfaces of layers are reactive to a wide range of organic molecules allowing the design of new materials through functionalization reactions for biological, catalysis or even environmental applications.

Double-layered hydroxides are one of the most important clays because of their adsorption capacity, functionalization, chemical stability, easy and economic synthesis, great biocompatibility, and therefore, a wide spectrum of possible applications.

Taking into account the principles of clays, double-layered hydroxides are a good option for bromate and chromate removal from aqueous solution, since both pollutants are found as oxyanions in water [47].

1.4.5.1.1 DLH Structure

From the materials chemistry perspective, the structure of double-layered hydroxides can be described from the magnesium hydroxide structure, commonly named as brucite. In brucite structure the basic units are sheets with Mg^{2+} cations placed in the middle and octahedrally coordinated by six hydroxyl groups. According with the second principle of Pauling, each Mg^{2+} cation shares its charges with six anions which provides +2/6 = +1/3 of charge; while each coordinated hydroxyl with three magnesium centers will provide -1/3 = -1/3 which results in a neutral overall electrostatic charge (+1/3-1/3=0) (see Figure 4) [1].

Double-layered hydroxides are the result of an isomorphic substitution of an “x” fraction of magnesium cations from a trivalent cation, thus generating positive charges in the sheets, which are offset with an interlayer anion. The general formula of double layered hydroxides is $[M^{2+}_{1-x} M^{3+}_{x} (OH)_2]^{x+} (A^{n-})_{x/n} \cdot mH_2O$; where M^{2+} is a divalent cation (Ca^{2+}, Mg^{2+}, Zn^{2+}, Co^{2+}, Ni^{2+}, Cu^{2+}, Mn^{2+}), M^{3+} is a trivalent cation (Al^{3+}, Cr^{3+}, Fe^{3+}, Co^{3+}, Ni^{3+}, Mn^{3+}), and A^n is an exchange anion (Cl^-, NO_3^-,

ClO_4^-, CO_3^{2-}, SO_4^{2-}). Cations used in synthesis of double-layered hydroxides are not limited only by divalent or trivalent anions, monovalent cations can be used (such as Li^+) and tetravalent cations (such as Ti^{4+}, Zr^{4+} and Si^{4+}), but thinner sheets structures are obtained than those with Mg/Al [47].

The x fraction of the trivalent cation determines the electrostatic charge of the sheet. Some natural clays have a fixed value of x=0.33, although the structure can be stable at values from 0.2 to 0.33. Even though double-layered hydroxides can be synthesized with x values out of this range, it is more probable that they have a different arrangement and also a decrease in crystallinity [46].

The x value affects also the interlayer distance and the ion exchange capacity. The size of cationic radios of M^{2+} and M^{3+} is an important parameter in the double-layered hydroxide synthesis because the isomorphic substitutions are ruled by ionic size and they also contain metals with similar cationic radii. Double-layered structures are flexible enough so any trivalent metal cation with a variation in ionic radio from 0.67 Å (Al^{3+}) to 0.93 Å (In^{3+}) can be in the structure, but they become unstable when the ionic radii of divalent metal cation is less than 0.6 Å. For a big divalent metal cation such as Ca^{2+} the arrangement turns to a hydrocalumite structure [48].

For hydrocalumite, the large difference of ionic radii (Ca^{2+}, 1.14 Å; M^{3+}, 0.56 a 0.64 Å) leads to strong distortions in the octahedral arrangement of a double-layered hydroxide to a heptahedral arrangement. For M^{3+}, large cations like Y^{3+} (1.04 Å) can be also destabilize the octahedral arrangement or even prevent this formation [49].

In the interlayer space, in addition to anions, water molecules are present and connected to both sheets and interlayer anions by hydrogen bonds, which are continuously breaking and mending, also water molecules are in a constant state of flux confirmed by nuclear magnetic resonance, so the interlayer zone is an extremely complex region.

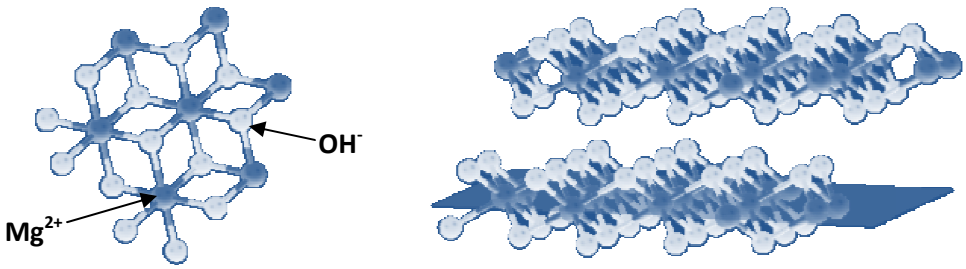

Figure 4 Brucite sheet section showing Mg^{2+} centers coordinated with six hydroxyl anions and each hydroxyl anion with three Mg^{2+} cations; also two brucite sheets which thickness corresponds to basal space [1].

1.4.5.1.2 Properties of DLH

Chemical stability is of great concern for most double-layered hydroxides purposes. The stability increases in the next order $Mg^{2+} < Mn^{2+} < Co^{2+} \approx Ni^{2+} < Zn^{2+}$ for divalent cations and $Al^{3+} < Fe^{3+}$ for trivalent cations. This is consistent with pK_{ps} of metal hydroxides being $Mg(OH)_2$ smaller than $Zn(OH)_2$. Double layered hydroxides containing Mg results more alkaline in aqueous solutions than double-layered hydroxides containing Zn [50].

The double-layered hydroxides thermal stability has been studied because most of the products obtained after thermal treatments are widely used in catalysis, biochemistry, water treatment, etc. even though a great number of metals can be used to synthesize double-layered hydroxides all of them have a similar behavior: 1) dehydration of interlayer water molecules, 2) chemical decomposition, losing hydroxyl groups attached to laminar cations and decomposition of interlayer anions, forming a mix of oxides, and 3) crystallization of the metal oxides. Researches have reported that thermal stability increases in the following order: Co/Al< Zn/Al≈ Cu/Al< Mg/Fe≈ Ni/Al< Mg/Al≈ Mg/Cr. Thermal decomposition in the oxides is moderately affected by the nature of the ions and interlayer molecules [51].

It has been tested that some anions turn double-layered hydroxides more stable in the dehydration step, while some organic molecules turn the sheets of a double-layered hydroxides to more expand or contracted ones in the same dehydration step [52].

1.4.5.1.3 Synthesis of DLH

Hidrotalcite is not a common structure in nature, but at laboratories and industries its synthesis is simple and low cost. Some of the used methods to synthesize double-layered hydroxides are the co-precipitation, urea method, memory effect, induced hydrolysis, sol-gel technique, electrosynthesis, and hydrothermal treatment methods, ultrasound and microwave, but one of the most practical methods is co-precipitation method.

Co-precipitation starts with the gradual and drop wise addition of an alkaline solution (NaOH, NH_4OH, or KOH) into a solution with two metal salts with a common anion. The most important parameters are pH, concentration of metal salts, washing, drying, and calcination temperature.

Some studies such as Crepaldi *et al.* showed that materials prepared by co-precipitation method developed a high crystallinity grade, low particle size, high surface area and high porous diameter, being important qualities for many technological applications [53].

To modify double-layered hydroxides by changing its interlayer anions, the ion exchange method is required. The process occurs by isomorphic substitutions of the interlayer anions while synthesis, which modifies the interlayer space between sheets; this process can be reversible using

chemical or thermal treatments. The preferential order for inorganic anions to be in the interlayer zone is: NO^{3-}< Br^{-}< Cl^{-}< F^{-}< OH^{-}< MoO_4^{2-}< SO_4^{2-}< CrO_4^{2-}< $HAsO_4^{2-}$< HPO_4^{2-}< CO_3^{2-}. Double-layered hydroxides have more affinity for multivalent or with more charge density anions because of great electrostatic interactions [1]. For this reason, the carbonate anion is strongly held by double-layered hydroxides. The ion exchange reactions are very simple and they consist in adding the double-layered hydroxides in a solution with the new anion, but it is necessary to have in solution an anion with more affinity than the original one. If the carbonate anion is not used in the synthesis, it is important to isolate the test so contamination with carbon dioxide which is oxidized to carbonate and create a competition with the rest of the anions. Both, co-precipitation and ion exchange methods are very simple and have a high efficiency in the incorporation of interlayer species [54].

1.4.5.1.4 Characterization of DLH

a) X Ray Diffraction (XRD)

Being a solid material, double-layered hydroxides can be study with different techniques to know their composition, properties and general characteristics. But, the most essential technique to obtain information about structure is XRD. A typical diffractogram where the small-angle reflection (2θ) corresponds to the reflection of basal plane (003), defined as the distance between two sheets analog to plane (001). The basal reflection (003) is the most intense one and if the double-layered hydroxide is very crystalline, it will be seen harmonic reflections at (006), (009),…, (00n), being n a multiple of 3; so, if the reflection (003) appears at 4 grades (2θ), the next reflections will appear at 8, 12,16, etc. [55].

The equation that shows the relation of the basal reflection with the distance between sheets is the Bragg equation [50]:

$$d_{hkl} = n\lambda/2sin\Theta \qquad (6)$$

If the value of basal distance is known, the interlayer space can be calculated if the thickness of a sheet is subtracted from the basal distance. The quality of sheet stacking can be observed in the reflections at 35 grades (2Theta) corresponding to plane (012), where the reflection is asymmetric and sometimes shows a sawtooth shape, this shows that when sheets are stacking they suffer a rotation over the c axis; but when the double-layered hydroxides are synthesize with a high crystalline quality, it can be observed that after 60 grades are one or two reflections in the diffraction profile, this one or two reflections are (110) and sometimes (113), which are equivalent to the distance between metal cations inside the sheets and the “a” cell parameter. With the distance of this plane the molar ratios can be verify, as the size of the crystallite by Scherrer equation:

$$\tau = \frac{K\lambda}{\beta cos\theta} \qquad (7)$$

Where K is a dimensionless shape factor, with a value close to unity. The shape factor has a typical value of about 0.9, but varies with the actual shape of the crystallite, τ is the mean size of the ordered (crystalline) domains, which may be smaller or equal to the grain size, λ is the X-ray wavelength, β is the line broadening at half the maximum intensity, after subtracting the instrumental line broadening, in radians. This quantity is also sometimes denoted as Δ (2θ), and θ is the Bragg angle.

Other characterization techniques are elemental analysis, differential thermal analysis (DTA), thermo-gravimetric analysis (TGA), nuclear magnetic resonance (NMR), and scanning electronic microscopy (SEM), among others. The selected techniques will vary depending of the information that wants to be obtained [56].

b) BET analysis

In physical gas adsorption, an inert gas (typically N_2) is adsorbed on the surface of a solid material. This occurs on the outer surface and, in case of porous materials, also on the surface of pores. Determination of the BET surface area by gas adsorption is well known. Adsorption of nitrogen at a temperature of 77 K leads to an adsorption isotherm, sometimes referred to as BET isotherm, mostly measured over porous materials.

The monolayer gas formation of molecules on the surface is used to determine the specific surface area, while the principle of capillary condensation can be applied to measure the presence of pores, pore volume and pore size distribution. Prior to the measurement, the sample is pre-treated at elevated temperature in vacuum or flowing gas in order to remove any contaminants [57].

c) Thermo-Gravimetric Analysis (TGA)

Thermo-gravimetric analysis (TGA) is a technique in which the mass of a substance is monitored as a function of temperature or time as the sample specimen is subjected to a controlled temperature program in a controlled atmosphere .TGA measures a sample's weight as it is heated or cooled in a furnace and it consists of a sample pan that is supported by a precision balance which resides in a furnace and is heated or cooled during the tests. The mass of the sample is monitored during the experiment. A sample purge gas controls the sample environment. This gas may be inert or a reactive gas (commonly N_2 or O_2) that flows over the sample and exits through an exhaust.

d) Scanning Electronic Microscopy (SEM)

A scanning microscope is provided for producing a scan image at high three-dimensional resolution and in a low acceleration voltage area. An acceleration tube is located in an electron beam path of an objective lens for applying a post-acceleration voltage of the primary electron beam. The application of an overlapping voltage onto a sample allows a retarding electric field against the primary electron beam to be formed between the acceleration tube and the sample. The secondary electrons generated from the sample and the secondary signals such as reflected electrons are extracted into the acceleration tube through the effect of an electric field (retarding electric field) immediately before the sample, then the signals are detected by a secondary signal detector located over the acceleration tube [58].

2 Background

2.1 Bromate removal methods

Because bromate is considered a carcinogenic compound, comprehensive studies had been developed to find the way bromate is formed in water after disinfection and to evaluate the effectiveness of bromate removal methods from water. In the following paragraphs some relevant studies are discussed briefly.

Liu *et al*. studied that not only ozonation but also chlorination can develop bromate formation. It has been confirmed that a few micrograms per liter of bromate can be found in waters if chlorination is used for final disinfection method and significant bromate formation in chlorinated water can be observed under some special conditions (*e.g*. sunlight irradiation). Bromate formation during chlorination is a slow process. In a first step, bromide is oxidized by hypochlorous acid (HOCl) to form hypobromous acid (HOBr) which is in equilibrium with OBr^-. Although there is no reaction between $HOCl/OCl^-$ and $HOBr/OBr^-$, HOBr can react to bromate and bromide and it is the reaction in which HOBr reacts with itself, leading to a reduced species and to oxidized species (*e.g*. BrO_3^-) [6].

In the case of bromate removal methods, Matos *et al*. studied the ion exchange method by using a membrane bioreactor to remove bromate from drinking water. Their results showed that in batch, system the biological reduction of bromate was slow and only occurs after the complete reduction of nitrate present in solution, but using anion exchange membranes showed that Donnan dialysis could efficiently remove bromate from polluted waters, this using samples of water containing 200 µg/L of BrO_3^- [16]. Similarly, Chitrakar *et al.* investigated the bromate uptake at trace levels with double-layered hydroxides. They reported that Fe-Al double-layered hydroxides could reduce bromate concentration from 100 µmol/L to 0.07 µmol/L, when a solid to liquid ratio of 1 g/L was used. Final bromate concentration corresponds to the maximum level established for drinking water, demonstrating that this adsorbent can be used in adsorption processes [46, 47]. In

contrast, Bhatnagar *et al*. tried granular ferric hydroxide for the removal of bromate from water in batch systems obtaining that the maximum adsorption capacity of this material was 16.5 mg/g. They studied the effect of initial bromate concentration, pH, contact time, temperature, and the presence of competing anions, but the effects of competing anions and solution pH were negligible for this adsorbent [59]. Finally, Tong-mian Liu *et al*. modified an activated carbon with nitric acid, sodium hydroxide and ammonia to evaluate the effect of these modifications on bromate removal in batch systems. They reported that ammonia treated activated carbon had the highest bromate adsorption capacity (1.55 mg/g) in comparison with the other treated adsorbents. A strong correlation was found between basic groups and adsorption capacity of bromate on modified carbons. In other words, enhancement of basic groups on activated carbons was favorable for bromate removal from aqueous solutions [60].

2.1.1 Bromate determination methods

Ion chromatography is the most widely used method for bromate determination because of its easy handling and not complex sample preparation. Bhatnagar *et al*. [59] used ion chromatography for bromate determination after adsorption process with granular ferric hydroxide, likewise, Tong-mian Liu et al. [60] used ion chromatography to determine final bromate concentration after adsorption with modified activated carbons.

The need to monitor bromate in ozonized drinking water at trace leves (ppb) has led researches to find alternative techniques. For instance, Day *et al*. showed that the instrumentation used in their study (HPLC-ICP-MS), achieved a detection limit of 0.14 ppb of bromate [61]. Similarly, Hatzistavros *et al*. developed a new method for determination of trace levels of bromates by selective membrane collection [62]. Several membranes containing a few micrograms of different complexing reagents in a poly(vinyl chloride) matrix were tested. At the first stage the prepared membranes collected both bromate and bromide ions, so different bromide masking agents were put in the analyzed solutions to avoid bromide collection. The minimum detection limit was equal to 1.0 µg/L for drinking water.

Some other methods had been developed for specific purposes based on ion chromatography. Cordeiro *et al*. used the ion chromatography method followed by post column reaction and ultraviolet detection where a pre-concentration step was not required [63]. The collaborative research investigated different types of drinking water such as soft drinking water, hard drinking water and mineral water. Test samples were sent to 17 laboratories in 9 different countries reaching a detection limit of 1.67 µg/L.

2.2 Chromate removal methods

Chromate is considered a carcinogenic compound and also it had been reported to cause several damages to human's health [10, 15, 24]as explained in section 1.2. For these reasons, researches had been developed new materials and tried a number of removal methods for this pollutant.

For instance, Leyva *et al*. studied the Cr(VI) adsorption by activated carbon fiber. The equilibrium adsorption data was obtained with the activated carbon fiber in a batch adsorber. The initial and final Cr(VI) concentration was determined by colorimetric method. In this study, researchers reported that Cr(VI)adsorption capacity decreased when the pH was increased from 4 to 10, but the adsorption capacity increased when temperature was raised from 15 to 35 °C. The adsorption capacity of Cr(VI) onto activated carbon fiber were compared with granular activated carbon of coconut and hazelnut finding that the adsorption capacity of the fiber was two folds of the hazelnut carbon and the half of coconut carbons [10].

Not only activated carbon, but also biomass has been tried to remove Cr (VI) from water as Kuo *et al*. studied. Cr (VI) uptake by impregnated shavings was high (1.18 µmol/g) [11]. Besides, Mohan *et al*. developed low cost adsorbents to remove tri- and hexavalent chromium from water using biomass and different activated carbons, being the dried anaerobic activated sludge the adsorbent with higher Cr (VI) adsorption capacity and the Amberlite IR-120 resin for Cr(III) [18].

2.2.1 Chromate determination method

The most common method for chromate determination in aqueous solutions is the colorimetric method by diphenylcarbazide coupled UV-vis spectrophotometry at 540 nm according to the method proposed on the Mexican norm NMX-AA-044-SCFI-2001.

2.3 Double-layered hydroxides structure

As it was mentioned in Section 1.4.5.1, double-layered hydroxides are synthetic structures comprising hydroxylated layers with positive electrostatic charges stabilized by interlayer anions. Being a complex structure, researchers had studied the structure of the double layered hydroxides to observe from a monocrystal the real structure of the complex compound. Arakcheeva *et al*. studied the crystal structure and chemistry of $Al_2Mg_4(OH)_{12}(CO_3)3H_2O$ (brucite), which is the double-layered hydroxide with Mg and Al as metal cations and carbonate as the exchanging anion [2]. Figure 5 shows the structure found by Arakcheeva *et al*. As it can be seen, the layers presented in the hydrotalcite-like compound are made of hydroxides of Mg and Al forming octahedral arrangement with water and anions are bonded together with the sheets.

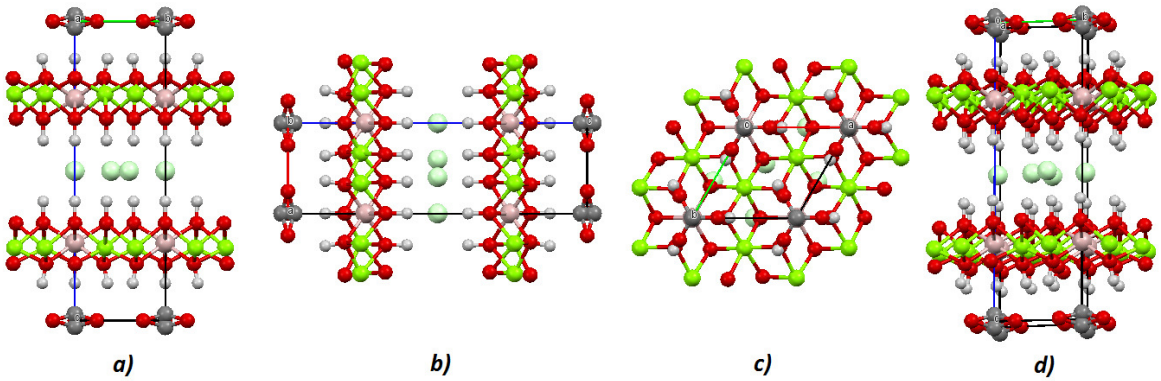

Figure 5 Structure of Mg/Al double-layered hydroxides with carbonate as the exchanging anion. a) view from plane a b) view from plane b, c) view from plane c and d) random view [2].

Moreover, properties, synthesis and characterization techniques for double-layered hydroxides were studied. Martínez *et al*. presented information about double-layered hydroxides in general, such as chemical structure, synthesis, characterization, and properties [1].

Aditionally, they also presented modification and possible application for double-layered hydroxides, for example: environmental remediation, catalysis, medicine and biology. For this project, environmental remediation with double-layered hydroxides has a great impact and covers a wide spectrum of pollutants removal, such as pathogen organisms (e.g. *E. coli*), heavy metals (Cu(II), Pb(II), etc.), anions (Cr(VI), As(V), F^-, I^-, BrO_3^-, etc.) and pesticides (2,4-D,MCPA, picloram 86, DNP and DNOC87).

Dongjuan *et al*. studied Mg/Fe double layered hydroxides for arsenate and fluoride removal indicating that the adsorbent present the highest adsorption capacity at 400°C. The study shows that adsorption capacities were closely related to the adsorbents structural properties developed during calcination [64].

2.4 Legal framework

In order to reduce the impact on human's health, a maximum allowed level of each pollutant (bromate and chromate) on drinking water had been established. In the next table, the maximum allowed levels are shown for the pollutants selected in this research. It is important to mention that regardless the agency (EPA, WHO, or NOM), bromate maximum level is the same 0.01 mg/L [9, 65, 66].

Table 1 Bromate and chromate maximum allowed level on drinking water by EPA, WHO and NOM.

Organization	Bromate maximum allowed level [mg/L]	Chromate maximum allowed level [mg/L]
EPA *U.S Environmental Protection Agency*	0.010	0.010
WHO *World Health Organization*	0.010	0.010
NOM *Normas Oficiales Mexicanas*	0.010	0.050

3 Research motivation

Since bromate and chromate are two carcinogenic compounds that could be found in drinking water risking human's health, efficient, economic and easy-to-do removal methods and adsorbents have to be developed. Double-layered hydroxides are adsorbents with a high adsorption capacity, an easy and non-risky synthesis, precursor salts are non-expensive reactants, and multiple adsorption/desorption cycles can be performed with the synthesized material. In fact, a wide variety of uses have been reported for double-layered hydroxides; for instance, the intensive use of double-layered hydroxides as adsorbents in removing diverse pollutant anions from aqueous solutions has been reported. However, there is a lack of information about the effect of thermal treatment of double layered hydroxides on the removal of anionic pollutants and, at the same time, adsorption/desorption and kinetic studies are not commonly reported for the dried and calcined adsorbents.

4 Hypothesis

Mg-Al double-layered hydroxides have an adsorption capacity greater than commercial granular activated carbon and they can be used for bromate and chromate removal in aqueous solution in batch and continuous process.

5 Objectives

5.1 General objective

To synthesize double-layered hydroxides (DLH) at different Mg/Al molar ratios to remove bromate and chromate from water by adsorption processes and to evaluate the effect of the drying step (100, 400, 500, and 600°C) on the adsorption of the target pollutants.

5.2 Specific objectives

a) To synthesize Mg-Al DLH by the precipitation method and to apply a different drying step for these materials (100, 400, 500 and 600°C).

b) To characterize the synthesized materials (Mg-Al DLH) before and after adsorption/desorption.

c) To conduct screening adsorption/desorption tests for all synthesized Mg-Al double-layered hydroxides to select the best adsorbents towards chromate.

d) To carry out chromate and bromate adsorption experiments in batch systems to obtain the isotherm parameters using the best DLH and activated carbon.

e) To perform chromate and bromate kinetic adsorption studies for the best adsorbent at different stirring speeds and methods (mechanical, magnetic, intermittent, and oscillatory mixing) to determine the required time to achieve the equilibrium as well as the adsorption capacity.

f) To conduct adsorption tests of chromate and bromate in continuous systems using a bed column packed with the best DLH to obtain the breakthrough curve.

6 Methodology

The experimental strategy in order to evaluate the removal of bromate and chromate from water using the Mg/Al DLH is described in the following sections.

6.1 Synthesis of Mg-Al Double-layered hydroxides with carbonate as the exchanging anion

To synthesize double-layered hydroxides, precursor salts with metallic cations of different charge values are needed. For this project, to synthesize Mg-Al double-layered hydroxides, $AlCl_3$ and $MgCl_2$ were used in order to supply metallic cations (Mg and Al) in the solution. The quantity of each salt is calculated by establishing selected molar ratios of Mg:Al (1:1 to 4:1) and an initial water volume. Table 2 shows the quantity in grams for each of the chosen molar ratios for 100 mL of water.

Table 2 Mass quantity per molar ratio of Mg: Al for 100 mL of water.

Salt	**Molar ratio Mg/Al**			
	1	**2**	**3**	**4**
$MgCl_2$ (g)	20.33	40.66	60.99	81.32
$AlCl_3$ (g)	24.143	24.143	24.143	24.143

Once that each of the quantity of salts per molar ratio were mixed with 100 mL of water, NaOH at 4 M was slowly added (in continuous vigorous mixing) until a pH of 9.5 was reached. Afterwards, suspension was stirred vigorously at 500 rpm for 6 hours at 70 °C to increase the collisions of molecules and promote the reaction of OH^- and Mg^{2+} and Al^{3+}. After the 6 hours, a solution of 50 mL of water with 10 g of Na_2CO_3 was added to the solution at pH 9.5. As soon as the Na_2CO_3 solution was added, the mixing velocity was set at the slowest velocity available in the magnetic stirrer for 24 hours at room temperature to promote the formation of flocs. After the 24 hours, Mg-Al double-layered hydroxides were formed, separated by filtration and solids were washed with deionized water until the pH of the water was equal to the initial pH of deionized water. Then, Mg-Al double-layered hydroxides were dried at 100°C for 12 hours. The final step was to grind the synthesized material into homogenous particles size [67].

6.2 Characterization of Mg-Al Double-layered hydroxides with carbonate as exchange anion

Characterization is required to determine DLH are formed with the selected Mg/Al molar ratios. By this far, four different adsorbents were synthesized. X-ray diffraction is the preferred technique to determine if the material presents a crystalline phase or it is completly amorphous; also, it can be seen which crystalline phases are present. X-ray diffractometers offer a wide data base which includes the chemical formula of each of the crystalline phases and they can be used to verify if each of the molar ratios were formed.

X-ray diffraction was used for all the synthesized adsorbents in a routine of 30 minutes from 5 to 90 degrees. Samples were provided as homogenous powder and they were identified throughout the document named as: DLH11100, DLH21110, DLH31100 and DLH41100, being:

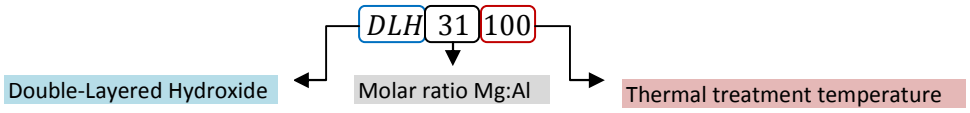

Once that the diffractograms of the samples were obtained, analyses by the evaluation program (EVA™) showed which of the synthesize adsorbents were formed with each of the proposed molar ratios.

Thermogravimetric analyses (TGA) of each of the adsorbents were conducted with oxidant atmosphere (O_2) starting at 25° C to 1000° C with a heating rate of 10°C/min. Samples were identified as above mentioned to identify in which temperature zone the structure starts to change.

6.3 Synthesis of Mg-Al Double-layered hydroxides with chloride as the exchanging anion

To synthesize DLH with chloride as the exchanging anion, Mg/Al molar ratio of 3 was selected because more ordered crystalline phases were detected by XRD analyses on DLH with carbonate. Synthesis procedure was similar as section 6.1, but no carbonate was added.

6.4 Characterization of Mg-Al Double-layered hydroxides with chloride as exchanging anion

The characterization of Mg-Al double-layered hydroxides with chloride as the exchanging anion by XRD and TGA were carried out as described in section 6.2.

Samples were provided as homogenous powder and they were identified as: DLHCL31100, being:

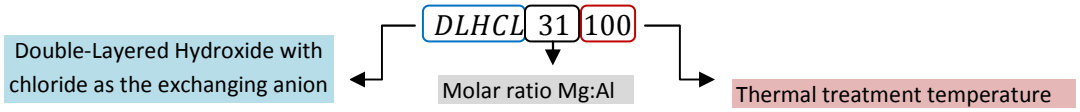

6.5 Calcination of Mg-Al Double-layered hydroxides

Calcination of the selected absorbents was performed at 400, 500 and 600°C and these samples were also characterized by XRD and TGA. These calcination temperatures were selected because it was reported thermal treatment (at 300°C or less) of double-layered hydroxides did not show pollutant adsorption [46], but recent studies have probed that higher temperatures enhanced pollutants adsorption [51, 46].

6.6 Characterization of calcined Mg-Al Double-layered hydroxides.

Characterization of calcined Mg-Al double layered hydroxides was conducted as shown in section 6.2.

6.7 Screening adsorption and desorption tests

Preliminary chromate equilibrium adsorption experiments in batch systems were carried out using all dried and calcined Mg/Al double layered hydroxides with carbonate and chloride as the exchanging anion.

Three stock solutions of chromate were prepared dissolving potassium dichromate salt as much as required in aqueous solutions to have an initial concentration of about 120 mg/L. Solution pH was adjusted to 6, 7 and 8 using 0.1 N solutions of HCl and/or NaOH as needed according the desired solution pH.

A volume of 25 mL of each stock was placed in 50 mL capped plastic and 25 mg of DLH adsorbent were added in each tube. Suspensions were continuously stirred and kept at 25°C for seven days. Finally, aliquots were withdrawn from the supernatant for measuring chromate at the equilibrium. Adsorption capacity was measured by using a mass balance in solution as shown in equation 1.

Desorption experiments were conducted by filtering the adsorbent after one week of adsorption. Samples of chromate-loaded DLH were placed in 50 mL capped plastic tubes with 25 mL of the desorption solution (containing 5 g/L of Na_2CO_3) and these suspensions were continuously stirred at 25 °C for 2 days. Aliquots were taken from supernatant after centrifugation and final chromate concentration was measured to determine desorption capacity using equation 1.

Initial and final concentration of chromate was performed by colorimetric method using diphenylcarbazide coupled to UV-vis spectrometer at 540 nm according to the method proposed on NMX-AA-044-SCFI-2001.

The first step of the chromate determination was to transfer 1 mL aliquot of each screening point into 25 mL volumetric flasks and then diluted with 0.1 N H_2SO_4 solution. Immediately, 0.5 mL of a diphenilcarbazide solution (25 mg of diphenilcarbazide diluted in 50 mL of acetone) was added to the solution and mixed vigorously to develop color. Five minutes later, absorbance of colored-solution was recorded at 540 nm by using UV-vis spectrophotometer.

These preliminary adsorption experiments will help to select those with higher chromate adsorption/desorption capacity. These selected adsorbents, will be used in adsorption experiments to build adsorption isotherms.

6.8 Additional characterization

Once adsorption tests were conducted, the adsorbents with higher adsorption capacity were selected and additional characterization to study surface area and structure was performed. The characterization methods that were used are: surface area analysis, scanning electron microscopy, X ray diffraction for after-adsorption-tests adsorbents with the use of Bragg's equation for the calculation of distance between sheets.

6.9 Chromate isotherms

The chromate adsorption capacity of DLH was determined at different pH values (6, 7 and 8) and experiments were conducted in duplicate, but average values are presented. Samples of 25 mg of adsorbent were added to 25 mL of chromate concentrations ranging from 25 to 500 mg/L. These experiments were continuously stirred at 150 rpm and temperature was kept constant at 25°C for seven days. The final pH was recorded once the equilibrium was achieved. The equilibrium was considered to be reached when at least 3 consecutive measurements of the chromate concentration were similar in the batch experiments. Aliquots were taken to measure the initial

and the equilibrium chromate concentrations as above described. Similar adsorption experiments were performed with commercial granular activated carbon for comparison purposes.

Experimental adsorption data helped to estimate parameters of isotherms for comparing with other adsorbent and, results also helped to evaluate the effect of pH on adsorption. Chromate adsorption, kinetic studies were conducted using the DLH with high adsorption/desorption capacity.

6.10 Bromate isotherms

The first step for bromate determination was to prepare bromate solution with concentration from 5 to 200 mg/L, then transfer 5 mL aliquots of each one into 5 mL ion chromatography (IC) plastic tube after centrifugation, and samples were placed at the IC autosampler. After this, each test were run taking 25 minutes to analyze each one, and bromate had a retention time in the IC column of about 11minutes [68].

Experimental adsorption data helped to estimate parameters of isotherms for comparing with other adsorbent and, results also helped to evaluate the effect of pH on adsorption. Bromate adsorption, kinetic studies were conducted using the DLH with high adsorption/desorption capacity.

6.11 Chromate kinetic studies

To conduct adsorption kinetic studies, four different mixing velocities were studied (100, 200, 300 rpm) using the system shown in Figure 6. A volume of 500 mL with a chromate concentration of 200 mg/L at pH 6 was added into a 1 L beaker. Then the beaker was settled in the mixing system showed in Figure 6. Subsequently, 500 mg of the selected adsorbent were added once that the system was mixing the chromate solution. Aliquots of 1 mL were taken from solution for measuring chromate concentration as above-mentioned.

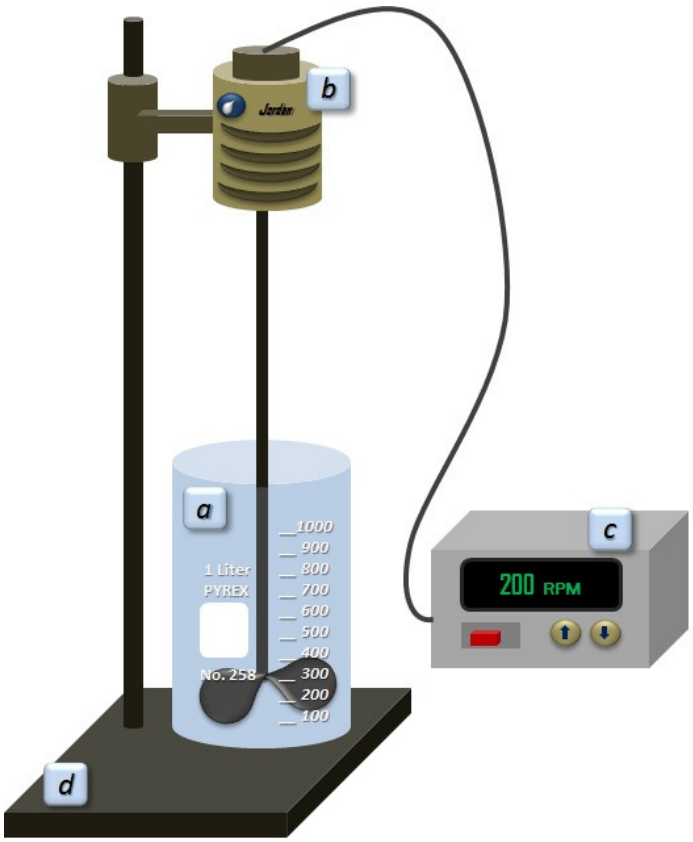

Figure 6 Kinetic studies mixing system. A) solution container (1 L beaker), b) vertical hollow shaft motor with 3 prop propeller of 3.5 cm each one, c) mixing speed controller (10-500 rpm) and d) 60 cm metallic motor holder.

6.12 Bromate kinetic studies

For bromate kinetic studies, the followed methodology is shown in section 6.10. An initial solution with a known concentration (C_o= 5 mg/L at room temperature) of bromate was prepared. Subsequently, 1.0 g of calcined double-layered hydroxide was placed in the solution until equilibrium was reached (168 h approx.) Determining the concentration of bromate was performed by ion chromatography.

The first step for bromate determination was to transfer 5 mL aliquots into 5 mL ion chromatography (IC) plastic tube after centrifugation, and samples were placed at the IC autosampler. After this, each test were run taking 25 minutes to analyze each one, and bromate had a retention time in the IC column of about 11minutes.

6.13 Packed bed column tests

In order conduct adsorption in continuous systems a packed bed column was built using 1.5 gr of the adsorbent with the highest adsorption/desorption capacity. It was necessary to find a particle

size where the solution could flow through the packed bed column without adsorbent loss. Different particle sizes were tested until a continuous flow was reached following the empty bed contact time (EBCT) optimal range. The flow rate was established at 0.5 mL/min at pH 6 at room temperature.

Once the adsorbent was fixed in the column, tests were conducted. Aliquots of 1 mL were taken from the treated effluent and the collected samples were analyzed to determine chromate and bromate concentration.

Determining the concentration of each taken aliquot was performed by colorimetric method coupled with UV-vis spectroscopy according to NMX-AA-044-SCFI-2001 for the chromate tests and ion chromatography for bromate tests.

6.14 Waste disposal

The Facultad de Ciencias Químicas of the Universidad Autónoma de Nuevo León and University of Texas at Arlington have the material and the correct administration for waste disposal for the generated wastes in this project like, industrial waste, glass and plastic with hazardous substances, highly toxic and carcinogenic solutions, inorganic salts solutions, etc.

7 Results

7.1 Synthesis of Mg-Al Double-layered hydroxides

7.1.1 DLH with carbonate as exchanging anion

As is explained in section 6.1, the synthesis of Mg-Al double layered hydroxides with carbonate as an exchange anion was performed obtaining four different adsorbents that in the next section their characterization is explained.

Figure 7 shows the four different Mg-Al double layered hydroxides with carbonate as the exchanging anion and they presented similar physical characteristics such as white coloration, and stone formation after the dehydration step. All adsorbents were grinded for the characterization and adsorption steps.

Figure 7 Mg-Al double-layered hydroxides with carbonate as exchanging anion with four different molar ratios. a) DLH1100, b) DLH21100, c) DLH31100, and d) DLH41100.

7.1.2 DLH with chloride as exchanging anion

Synthesis of Mg-Al double layered hydroxides with chloride as exchanging anion was performed using Mg/Al ratio of 3 based on previous results.

In Figure 8, the Mg-Al double layered hydroxides with chloride as the exchanging anion and they presented similar physical characteristics than DLH shown in Figure 7.

Figure 8 Mg-Al double-layered hydroxides with chloride as exchange anion with best molar ratio (DLHCL31100).

7.2 Characterization of Mg-Al Double-layered hydroxides

7.2.1 X ray diffraction (XRD)

Diffractograms of the four dried DLH with carbonate as exchanging anion were obtained by XRD, and they presented similar patterns in their planes, but different crystallinity level due to the Mg quantity in their sheets. As it was explained by Martinez *et al*. most stables hydrotalcite-like compounds have a fixed value of x=0.33 (x is the fraction of sides occupied by the trivalent metal cation) which means that the best Mg/Al molar ratio is at 3:1 [1]. Also, to verify the synthesized Mg-Al double layered hydroxides with chloride as exchanging anion XRD was used.

Figure 9 shows XRD patterns of dried Mg-Al double-layered hydroxides with carbonate and chloride as exchanging anions. It can be seen that the adsorbents have symmetric reflections for (003), (006), (009) and (012) planes and broad asymmetric peaks for (110) and (113) planes, which are characteristics for hydrotalcite-like compounds [2]. Some differences can be observed, like background noise due to low crystallinity development with respect to the molar ratio of Mg/Al. The sharpness and intensity of the reflections, as a measure of crystallinity, increased with the addition of Mg^{2+} ions. Furthermore, an increment of magnesium quantity led to a higher degree of crystallinity and better layered structure of samples and the stronger X-ray reflections were observed until Mg/Al molar ratio of 3 (x=0.33) was used for synthesis.

Table 3 Phases present in each sample of Mg-Al double layered hydroxides by XRD.

Sample	Present crystalline phases
DLH11100	$Mg_4Al_2(OH)_{14}{\cdot}3H_2O$, $((Mg_4Al_2)(OH)_{12}CO_3(H2O)_3)_{0.5,}$ $Al(OH)_3$
DLH21100	$Mg_4Al_2(OH)_{14}{\cdot}3H_2O$, $((Mg_4Al_2)(OH)_{12}CO_3(H2O)_3)_{0.5}$
DLH31100	$Mg_6Al_2(OH)_{18}{\cdot}4.5H_2O$, $((Mg_4Al_2)(OH)_{12}CO_3(H2O)_3)_{0.5}$
DLH41100	$Mg_6Al_2(OH)_{18}{\cdot}4.5H_2O$, $((Mg_4Al_2)(OH)_{12}CO_3(H2O)_3)_{0.5}$
DLHCL31100	$Mg_6Al_2(OH)_{18}{\cdot}4.5H_2O$

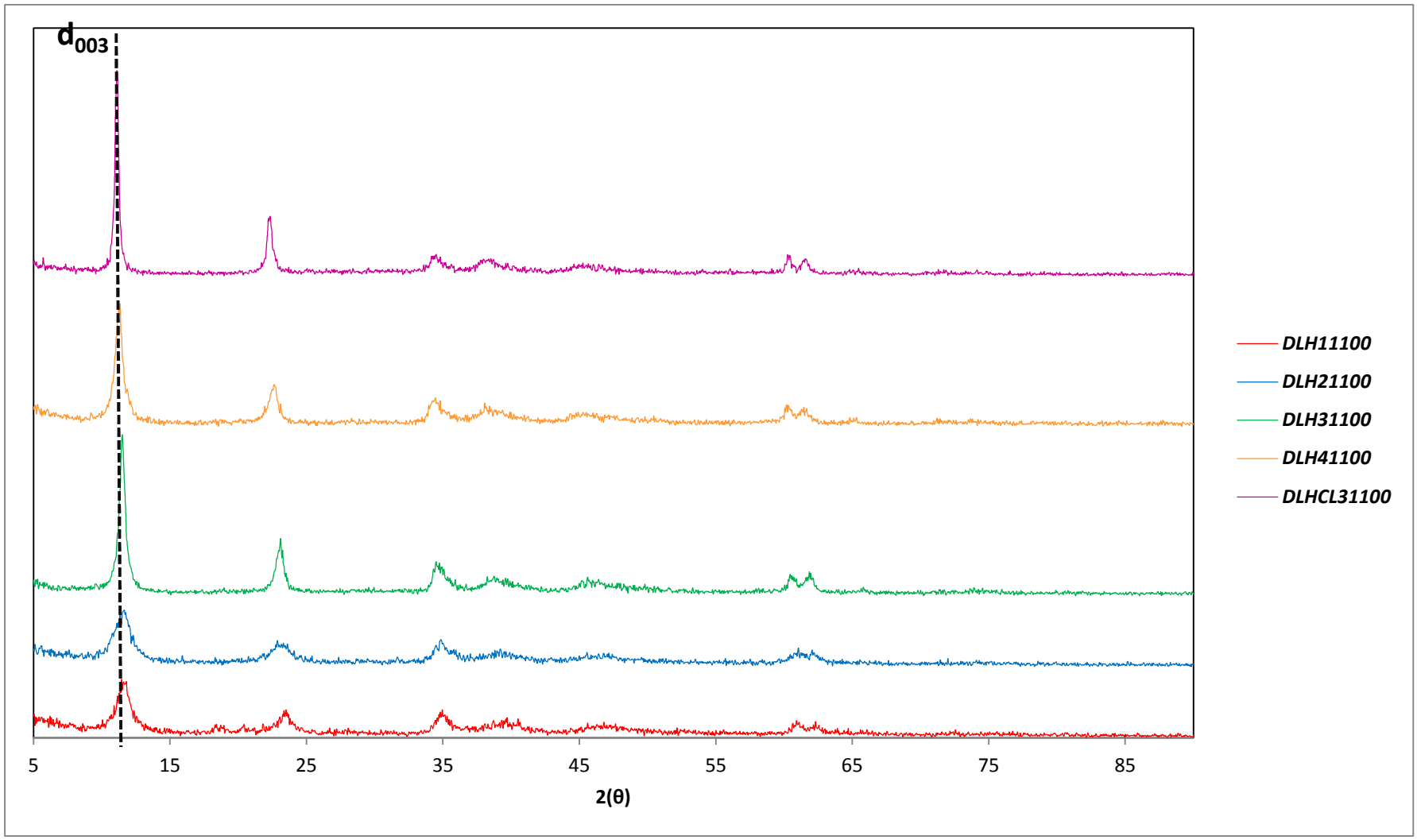

Figure 9 X-ray diffractograms of dried Mg-Al double layered hydroxides at different Mg/Al molar ratio (1 to 4) with carbonate and chloride as exchanging anions.

The crystalline phases present from comparison of diffractograms with EVA™ software database are shown in Table 3.

The identified phases match with the theoretical phases wanted for this research, but the only two adsorbents that reached the established molar ratios were DHL21100, DLH31100 and DLHCL31100. Similary, intensity of peaks on diffractograms helped to select the adsorbent with best chemical conditions such as high level of crystallinity. Arakcheeva and Pushcharovsky (1996) studies found that hidrotalcite-like compounds are synthesized as layered compounds.

X-ray diffraction patterns, shown in Figure 9, display phases corresponding to the DLHs. The position of the basal peaks of DLHs indicates the distance between two adjacent metal hydroxide sheets (003). The d-spacing is calculated using Bragg's equation:

$$d_{hkl} = n\lambda/2sin\Theta \qquad (6)$$

Where k is the X-ray wavelength (1.5406$\dot{A}$). The calculated d-spacing value (from 2θ value of 11.42°) was 7.01 Å, which corresponds to the thickness of the layers as well as the size of the anion and the water molecules existing in the interlayer [50], so if the height of the layer (4.77 Å) is subtracted, the height of the interlayer zone could be calculated which was 2.24 Å for carbonate as exchanging anion; for chloride exchanging anion the d–spacing value was 8.40 Å and the height of the interlayer zone was 3.63 Å corresponding to chloride ion as its shown in Figure 10.

2.1.1 Thermogravimetric analysis

The thermogravimetric analyses (TGA) showed that DLHs present three stages of weight loss upon heating between 25-1000 °C (Figure 11): the first stage from room temperature to approximately 225 °C can be attributed to the removal of surface adsorbed water and interlayer water molecules [51], the second step (225-500 °C) involves a gradual weight loss of the deintercalation of carbonate and dehydroxilation of the brucite-like layers (mixed oxides formation), and a third step (500-1000 °C) is assigned to a stage of stable oxides formation that present no memory effect (no adsorption capacity) [69]. Memory effect is the ability that a body or molecule can have to return to the initial structure after it has been exposed to stress, tension or temperature. In the case of DLH the initial structure of the molecule is form by sheets of magnesium and aluminum hydroxide which with high temperature (400 °C - 600 °C) is lost, nevertheless DLH present memory effect in solution with anions [2].

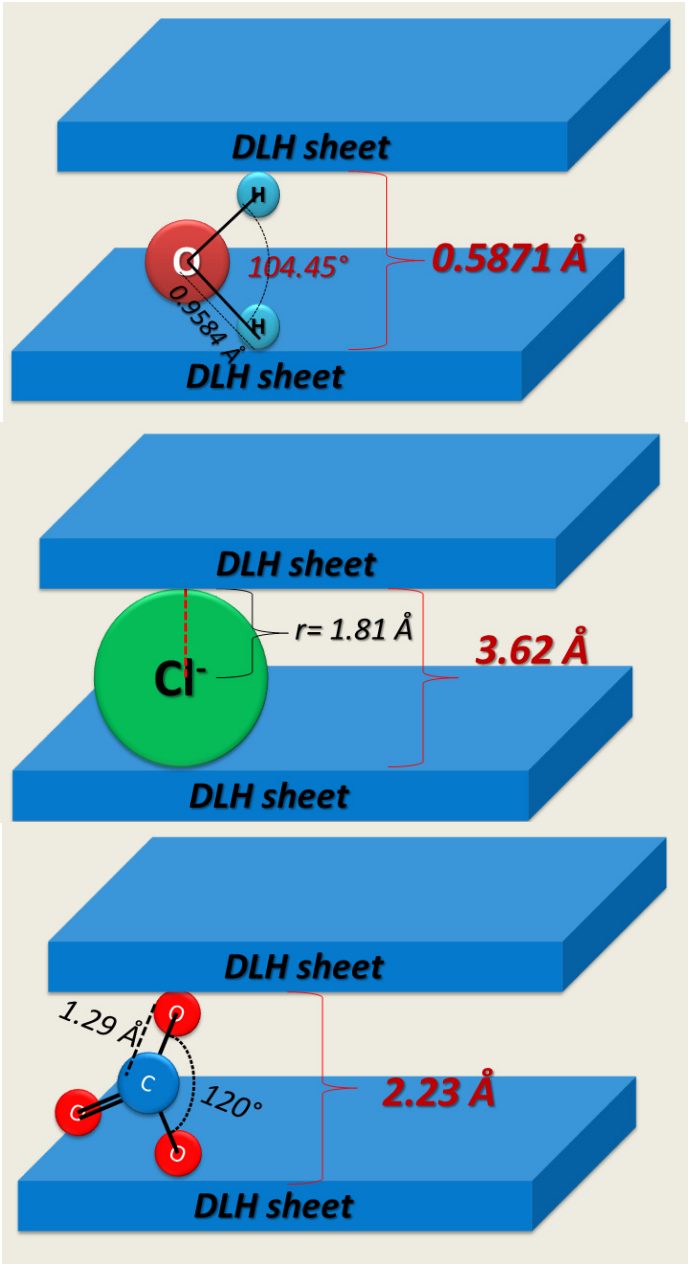

Figure 10 Water and exchanging anions bonded to DLH sheets.

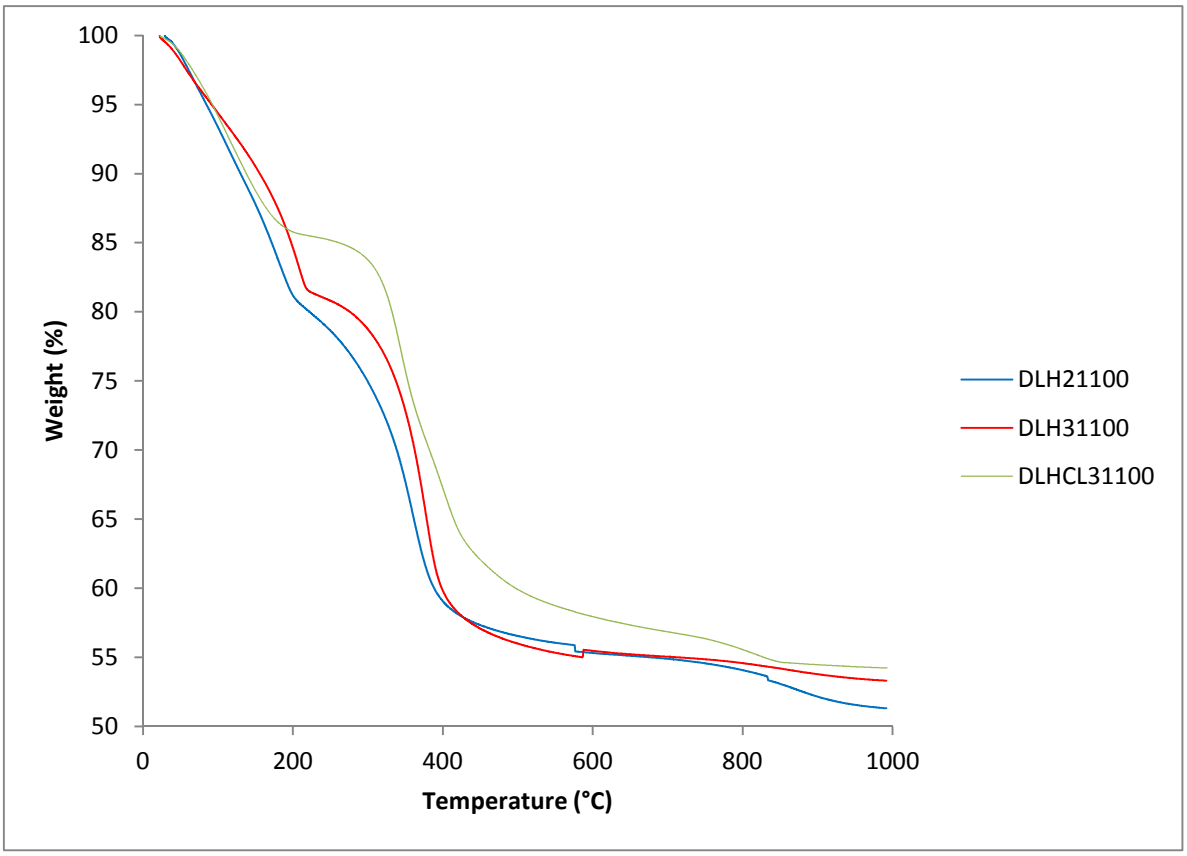

Figure 11 Thermogravimetric analyses of DLH21100, DLH31100 and DLHCL31100.

2.2 Calcination of Mg-Al Double-layered hydroxides

Even though Mg/Al molar ratio with highest crystallinity and layer order is 3, molar ratio of 2 was also selected to evaluate their chromate adsorption capacities using carbonate and chloride as the exchanging anion. In other words, three different adsorbents (DLH21100, DLH31100 and DLHCL31100) were calcined at 400, 500 and 600 °C.

In Table 4, the weight loss of DLH after calcination is presented. After calcination, the appearance of solids did not change as observed in Figure 11, but average weight loss achieved about 40% after thermal treatment. Weight loss was similar for all materials despite different weight loss.

According to literature and XRD characterization results, at low thermal treatment calcination (<400°C) the metal mixed oxides cannot be formed whish in not favorable for adsorption by memory effect, but a high calcination temperature could lead to formation of stable phases of metal oxides so the adsorption by reconstruction of double-layered hydroxides cannot be performed, so higher temperature (>400°C) was studied to find the temperature with the highest adsorption capacity. Also, the reconstruction occurred at specific temperatures range to achieve thermal decomposition and expose the interlayer zone with available adsorption sites [46].

Figure 12 Mg-Al double-layered hydroxides at 400, 500 and 600 °C. a) DLH21400, b) DLH21500, c)DLH21600, d)DLH31400, e)DLH31500, f) DLH31600, g) DLHCL31400, h) DLHCL31500 and i) DLHCL31600

Table 4 Weight loss of DLH after calcination.

Initial Sample	Calcination Temperature [°C]	Initial weight [g]	Final weight [g]	Weight loss [%]
HDL21100	400	1.0005	0.627	37.35
	500	1.0004	0.6293	37.11
	600	1.0004	0.6121	38.83
HDL31100	400	1.0009	0.6040	39.69
	500	1.0004	0.5959	40.45
	600	1.0009	0.5868	41.41
HDLCL31100	400	1.0005	0.6070	39.95
	500	1.0004	0.5962	40.42
	600	1.0004	0.5865	41.39

2.3 Characterization of calcined Mg-Al Double-layered hydroxides.

Remarkable differences of X-ray diffractogram patterns were detected for all Mg-Al double layered hydroxides calcined from 400 to 600 °C. After calcination step, the well-defined peaks of dried samples were replaced by broad peaks indicating that structure of the double-layered hydroxides was mainly destroyed and layers collapsed. The broad peaks suggest an amorphous phase and the presence of a mixture of magnesium and aluminum oxides by losing interlayer anions (mainly chemisorbed water molecules) [2].

Table 5 shows the compounds found in the samples after calcination. Samples with calcination temperatures of 100 °C shows the crystalline phase of a double-layered hydroxide, after calcination at 400, 500, and 600 °C the X-ray diffractometer showed that structure was lost and magnesium and aluminum oxides were formed.

After calcination, a mixture of metal oxides is found (AlO and MgO). The mixture of metal oxides found on the matrix depends on the molar ratio (Mg:Al) of the DLH, if the molar ratio is high (*i.e.* 3:1) the metal oxide with the fewest number of sites (Al) seemingly cannot be set apart by the X ray diffractometer evaluator.

Table 5 Phases present in each sample of Mg-Al double layered hydroxides by XRD.

Sample	Present crystalline phases
HDL21100	**$(Mg_4Al_2(OH)_{14} \cdot 3H_2O$, $((Mg_4Al_2)(OH)_{12}\cdot CO_3\cdot 3(H_2O)3)_{0.5})$**
HDL21400	**(AlO,MgO)**
HDL21500	**(AlO,MgO)**
HDL21600	**(AlO, MgO)**
HDL31100	**$(Mg_6Al_2(OH)_{18} \cdot 4.5\ H_2O$, $(Mg_4Al_2)(OH)_{12}\cdot CO_3\cdot (H_2O)_3)$**
HDL31400	**MgO**
HDL31500	**MgO**
HDL31600	**MgO**
HDLCL31100	**$(Mg_6Al_2(OH)_{18} \cdot 4.5\ H_2O$, $(Mg_4Al_2)(OH)_{12}\cdot CO_3\cdot (H_2O)_3)$**
HDLCL31400	**MgO**
HDLCL31500	**MgO**
HDLCL31600	**MgO**

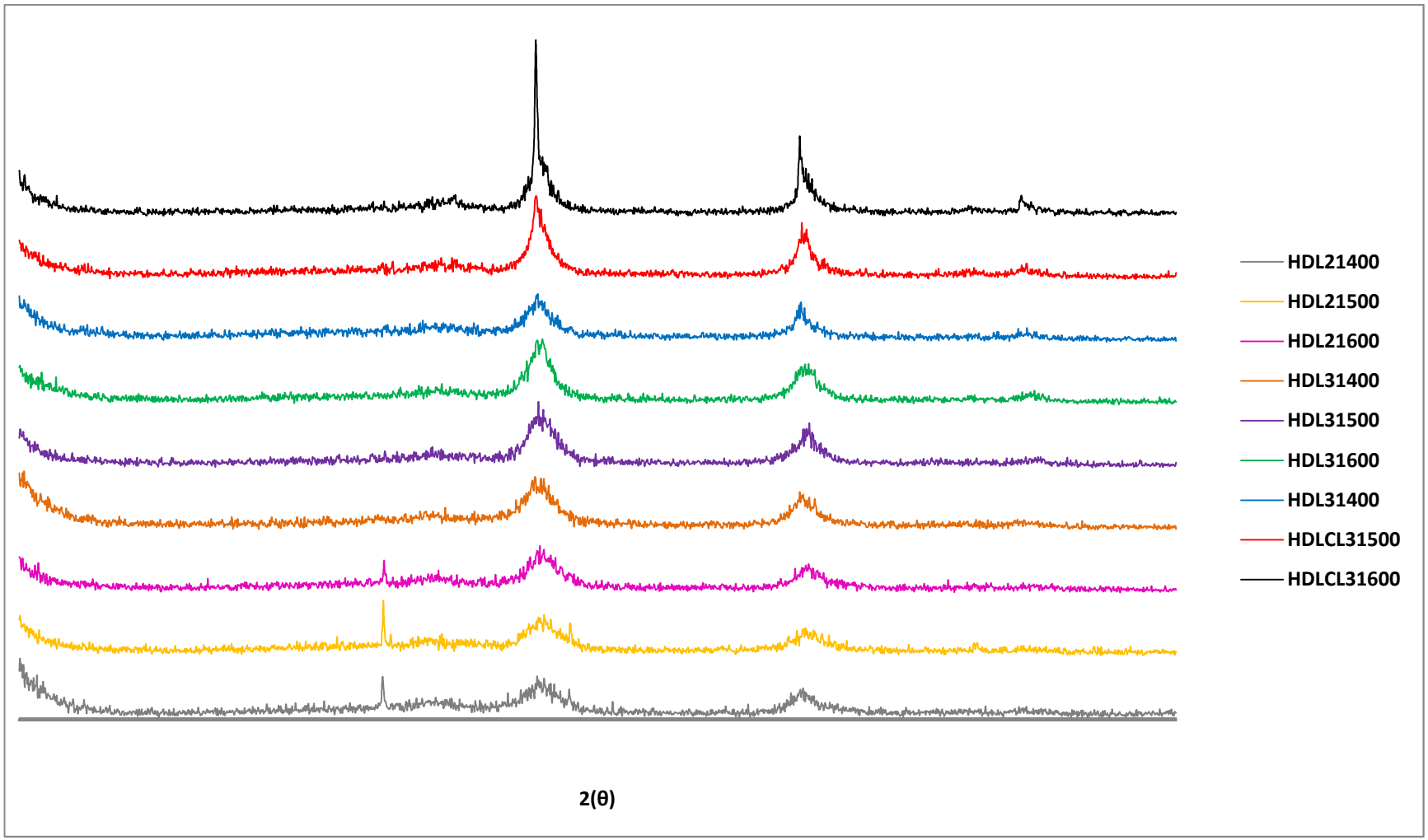

Figure 13 X-ray diffractograms of Mg-Al double layered hydroxides at different Mg/Al molar ratio (1 to 4) with carbonate and chloride as exchanging anions at 400, 500 and 600°C.

2.4 Screening adsorption and desorption tests

Once adsorbents were synthesized and characterized, a screening adsorption test was carried out to determine the chromate adsorption capacity of these materials.

Each of the adsorbents was tested at pH 6, 7, and 8. These values were selected so information for real drinking water (around pH values of 7) is available and also if solutions are too alkaline they will have many hydroxyl groups that can compete for adsorption sites. Also while HCl or NaOH is added to the solutions to establish the pH, Cl^- and OH^- are added which can create competition with bromate and chromate ions, so the less quantity of HCl and NaOH added the better. Table 6 shows the results of the screening tests for each adsorbent, thermal treatment temperature and pH values.

Table 6 Screening chromate adsorption tests.

No.	Compound	Molar ratio (Mg/Al)	Exchange anion	Thermal treatment temperature (°C)	pH	q_{ads} (mg/g)	q_{des} (mg/g)
1	CAGC	/	/	/	6	47.26	29.06
2	CAGC	/	/	/	7	21.72	7.74
3	CAGC	/	/	/	8	11.50	6.19
4	HDL	(2:1)	CO_3^{-2}	100	6	14.05	6.98
5	HDL	(2:1)	CO_3^{-2}	100	7	20.44	5.28
6	HDL	(2:1)	CO_3^{-2}	100	8	22.35	4.84
7	HDL	(2:1)	CO_3^{-2}	400	6	116.69	63.80
8	HDL	(2:1)	CO_3^{-2}	400	7	116.94	53.40
9	HDL	(2:1)	CO_3^{-2}	400	8	119.88	47.18
10	HDL	(2:1)	CO_3^{-2}	500	6	115.73	64.14
11	HDL	(2:1)	CO_3^{-2}	500	7	117.64	56.26
12	HDL	(2:1)	CO_3^{-2}	500	8	119.50	67.63
13	HDL	(2:1)	CO_3^{-2}	600	6	115.73	63.20
14	HDL	(2:1)	CO_3^{-2}	600	7	115.86	63.28
15	HDL	(2:1)	CO_3^{-2}	600	8	117.90	67.16

16	HDL	(3:1)	CO_3^{-2}	100	6	42.54	12.88
17	HDL	(3:1)	CO_3^{-2}	100	7	43.43	13.26
18	HDL	(3:1)	CO_3^{-2}	100	8	37.04	10.94
19	HDL	(3:1)	CO_3^{-2}	400	6	107.39	28.70
20	HDL	(3:1)	CO_3^{-2}	400	7	107.60	25.20
21	HDL	(3:1)	CO_3^{-2}	400	8	110.35	26.26
22	HDL	(3:1)	CO_3^{-2}	500	6	116.62	66.66
23	HDL	(3:1)	CO_3^{-2}	500	7	119.18	73.00
24	HDL	(3:1)	CO_3^{-2}	500	8	121.09	65.74
25	HDL	(3:1)	CO_3^{-2}	600	6	117.52	68.28
26	HDL	(3:1)	CO_3^{-2}	600	7	119.43	48.12
27	HDL	(3:1)	CO_3^{-2}	600	8	121.22	57.86
28	HDL	(3:1)	Cl^-	100	6	100.91	7.04
29	HDL	(3:1)	Cl^-	100	7	101.55	5.50
30	HDL	(3:1)	Cl^-	100	8	107.30	12.66
31	HDL	(3:1)	Cl^-	400	6	102.39	25.92
32	HDL	(3:1)	Cl^-	400	7	103.41	36.44
33	HDL	(3:1)	Cl^-	400	8	106.16	25.1
34	HDL	(3:1)	Cl^-	500	6	111.18	67.28
35	HDL	(3:1)	Cl^-	500	7	114.24	74.20
36	HDL	(3:1)	Cl^-	500	8	115.71	72.69
37	HDL	(3:1)	Cl^-	600	6	100.47	65.58
38	HDL	(3:1)	Cl^-	600	7	104.24	71.42
39	HDL	(3:1)	Cl^-	600	8	107.11	63.82

The adsorption tests described in Table 6 showed that the best adsorbent (higher adsorption and desorption capacities) were the double-layered hydroxides with Mg/Al molar ratio of 3:1 (DLH31500) with carbonate as exchange ion, and a thermal treatment temperature of 500 °C, having adsorption capacities between 116.62 mg/g (initial concentration of 117.13 mg/L) and 121.09 mg/g (initial concentration of 121.57 mg/L) and desorption capacities of 66.66 mg/g (116.62 mg/g) and 65.74 mg/g (121.09 mg/g).

Some other adsorbents with good performance were double-layered hydroxides with molar ratio of 3:1 with carbonate as exchange anion and thermal treatment temperature of 600 °C, having adsorption capacities between 117.52 mg/g (initial concentration of 117.13 mg/L) and 121.22 mg/g (initial concentration of 121.57 mg/L) and desorption capacities of 68.28 mg/g (115.62 mg/L) and 57.86 mg/g (121.57 mg/L); also double-layered hydroxides with molar ratio of 3:1 with chloride as exchange anion and thermal treatment temperature of 500 °C, having adsorption capacities between 111.18 mg/g (initial concentration of 117.13 mg/L) and 115.71 mg/g (initial concentration of 121.57 mg/L) and desorption capacities of 67.28 mg/g (115.62 mg/L) and 72.78 mg/g (120.75 mg/L); also double-layered hydroxides with molar ratio of 3:1 with chloride as exchange anion and thermal treatment temperature of 600 °C, having adsorption capacities between 100.47 mg/g (initial concentration of 117.13 mg/L) and 107.11 mg/g (initial concentration of 121.57 mg/L) and desorption capacities of 65.58 mg/g (115.62 mg/L) and 63.82 mg/g (120.75 mg/L).

The adsorbents with higher adsorption capacities were the material with thermal treatment of 500 and 600 °C, this can be explained with the thermogravimetric analysis of an DLH that shows three stages related to weight loss and structure variation, the first stage (from 25 °C to 225 °C) is when the removal of surface water and interlayer water molecules occurs, the second stage (from 225 °C to 600 °C) is related to the deintercalation of carbonate and dehydroxilation of the brucite-like layers and the third stage (from 600 °C to 1000 °C) has no adsorption capacity due to the formation of stable oxides which do not react with available anions present in the solutions.

So the four selected adsorbents were DLH31500, DLH31600, DLHCL31500, and DLHCL31600 and with them, isotherms were performed at pH 6, 7 and 8 to calculate their adsorption capacities and best pH condition.

2.5 Additional characterization

Once adsorption tests are done, the best adsorbents were chosen and additional characterization was conducted in order to describe the materials widely by surface area analysis and scanning electron microscopy.

2.5.1 Surface area analysis

Table 7 shows the Branauer-Emmet-Teller (BET) and Barrer-Joyned-Halena (BJH) analysis for surface area and pore distribution.

Table 7 Surface area values for the selected DLH.

Adsorbent	Surface area (m^2/g)	Pore volume (cm^3/g)	Pore diameter (Å)	Micropores (%)	Mesopores (%)	Macropores (%)
DLH31100	12.05	0.170	198.17	0.00	64.86	35.14
DLH31500	38.28	0.460	150.40	0.00	68.80	31.20
DLH31600	83.87	0.760	142.12	0.00	60.86	39.14
DLHCL31100	53.78	0.663	334.40	0.36	31.73	67.91
DLHCL31500	95.11	1.060	295.24	0.07	33.89	66.04
DLHCL31600	166.93	1.150	284.21	0.11	32.58	67.31
CGAC	753.50	3.870	17.35	8.17	88.47	3.36

With the Branauer-Emmet-Teller analysis (BET) and Barrer-Joyned-Halena (BJH) the surface area and pore distribution could be analyzed. It can be seen that the surface area was increased at higher calcination temperatures which is attributed to the collapse of layer and the conversion from DLH to magnesium and aluminum mixed oxides, this because DLH can stack on top of each other to build a three-dimensional network and are held together by hydrogen bonding between the sheets but when the calcination break the most of network it unravels, increasing the available superficial area. Nevertheless, with the increase of calcination temperature, pore diameter decreased because when the network unravels, the exchanging anions start to leave the interlayer zone, changing the distance between sheets. [64]

For DLH with carbonate as exchanging anion the pores are mainly mesopores, and for DLH with chloride as exchanging anion are macropores, due to the size of exchanging anion and the way they are bonded to the sheets (see Figure 10).

2.5.2 Scanning electron microscopy

The images produced by SEM for the best adsorbent (uncalcined, calcined and post-adsorption) are shown next. Chemical analysis is also used with the SEM technique be able to know the chemical composition of the materials.

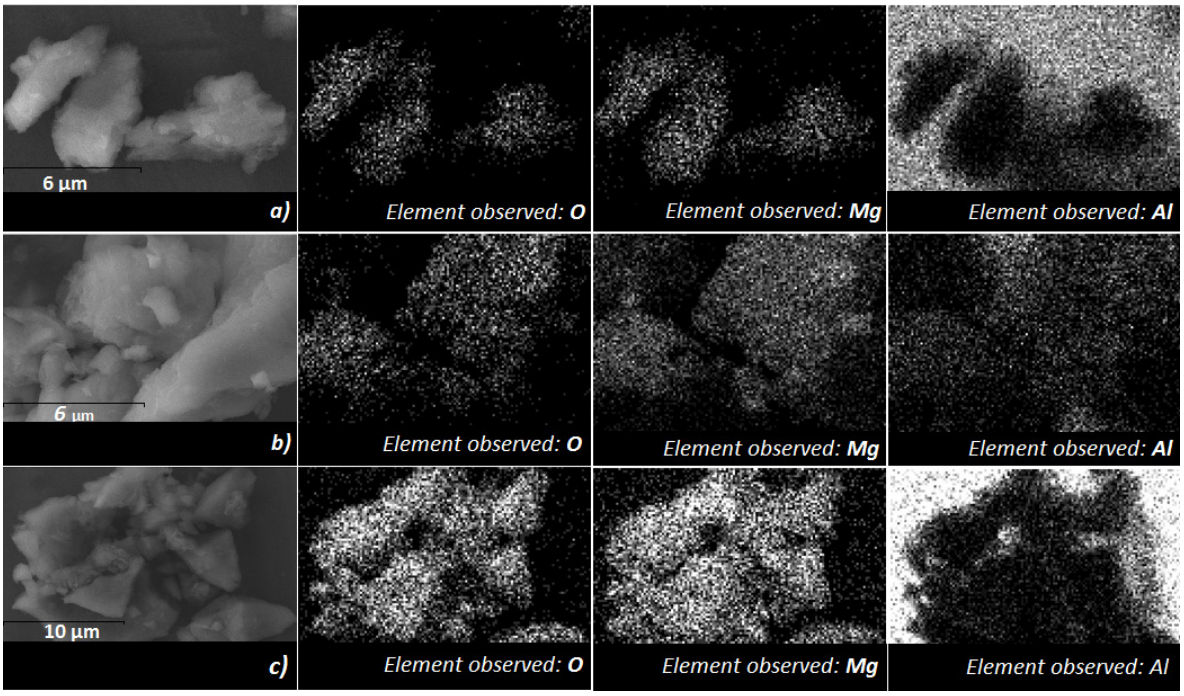

Figure 14 SEM images for a) DLH31100 b) DLH31500 c) DLH31500 after chromate adsorption.

Even though SEM is a punctual analysis (microscopic zones are studied), the presented images are a general representation of all the images obtained in the microscopy, finding that samples contain oxygen, magnesium and aluminum. As it can be seen, aluminum was used as support in the background so it appears in the sample and more in the opposite side (support).

In SEM analyses, a chemical analysis can be done, which provided of numerical data of the given sample (weight percent and atomic percent). For this research, the selected adsorbent (material with the highest capacity) was study as Figure 14 shows (before calcination, after calcination, and after chromate adsorption). Table 8 shows the weight and atomic percent of all the elements found in each sample.

It has to be considered that aluminum is present in less quantity if the presence of the SEM support is subtracted. SEM and its chemical analyses helped to reinforce the elements found in XRD individually.

Table 8 Weight and atomic percent for the selected DLH after chromate adsorption.

Sample	Element	Weight %	Atomic %
DLH31100 (Dried)	***C***	6.16	11.04
	O	25.72	34.61
	Mg	4.74	4.2
	Al	60.91	48.6
	Cl	2.18	1.33
	Si	0.29	0.22
Total		100	100
DLH31500 (Calcined)	***C***	3.36	6
	O	35.33	47.36
	Mg	4.08	3.59
	Al	4.47	3.56
	Na	13.27	12.38
	Cl	11.92	7.2
	Si	22.58	17.24
	Ca	4.99	2.67
Total		100	100
DLH31500 (Calcined and after adsorption)	***C***	9.75	15.63
	O	39.86	47.96
	Mg	9.28	7.35
	Al	40.23	28.71
	Cl	0.17	0.09
	Cr	0.71	0.26
Total		100	100

2.5.3 XRD after chromate adsorption

X-Ray diffraction analysis was conducted after adsorption of chromate oxyanions to verify if the adsorption is occurring by a memory effect (layers reconstruction by anion adsorption). With the diffractogram of the sample with adsorbed chromate, calculation for the interlayer distance was conducted.

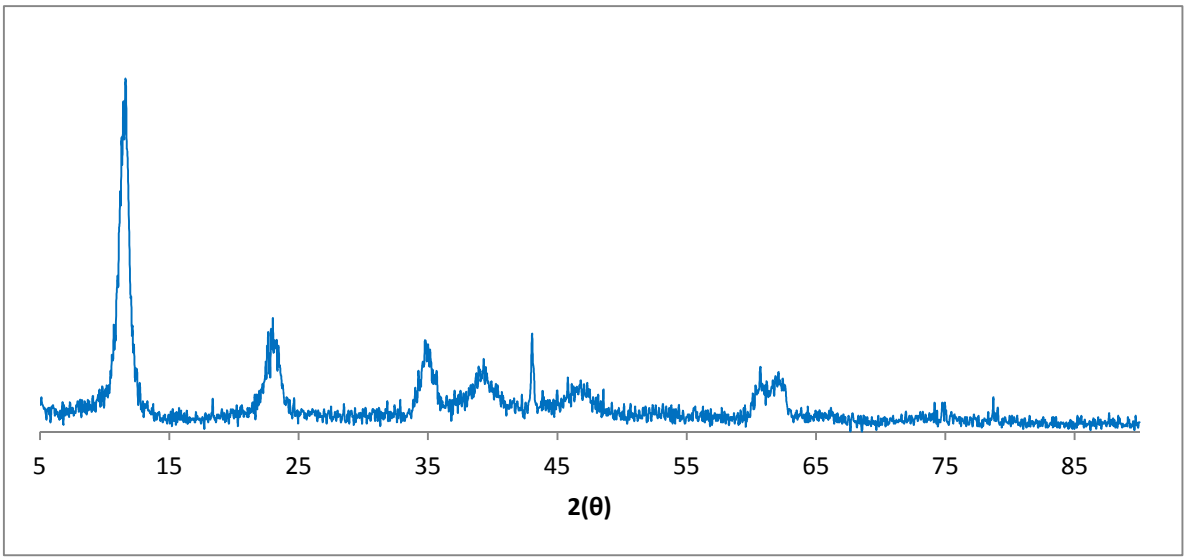

Figure 15 XRD diffractogram for DLH31500 after chromate adsorption at pH 6.

As it was calculated in section 7.2.1, the d-spacing value (2θ of 11.60°) after chromate adsorption by Mg-Al DLH was 7.50 Å and if the height of the layer (4.77 Å) is subtracted, the distance between sheets was 2.73 Å which corresponds to chromate ion. This result shows that the chromate ion was adsorbed between layers of the double-layered hydroxides as it was stated.

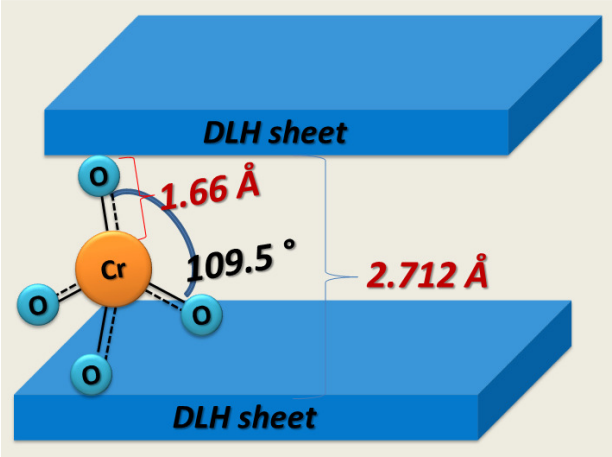

Figure 16 Chromate anion bonded to DLH sheets.

2.6 Chromate isotherms

As it is explained in section 7.7 isotherms for the best four adsorbents were performed in order to calculate their maximum adsorption capacities and the pH condition where they would present the highest capacity.

Figures 7.11, 7.12, 7.13, and 7.14 show the isotherms for each of the adsorbents and also the isotherm of commercial granular activated carbon at its best pH condition (notorious highest adsorption at pH 6 in screening tests).

At pH 6 maximum adsorption capacities were reached. This is due to the low presence of hydroxile groups competing with the chromate ion.

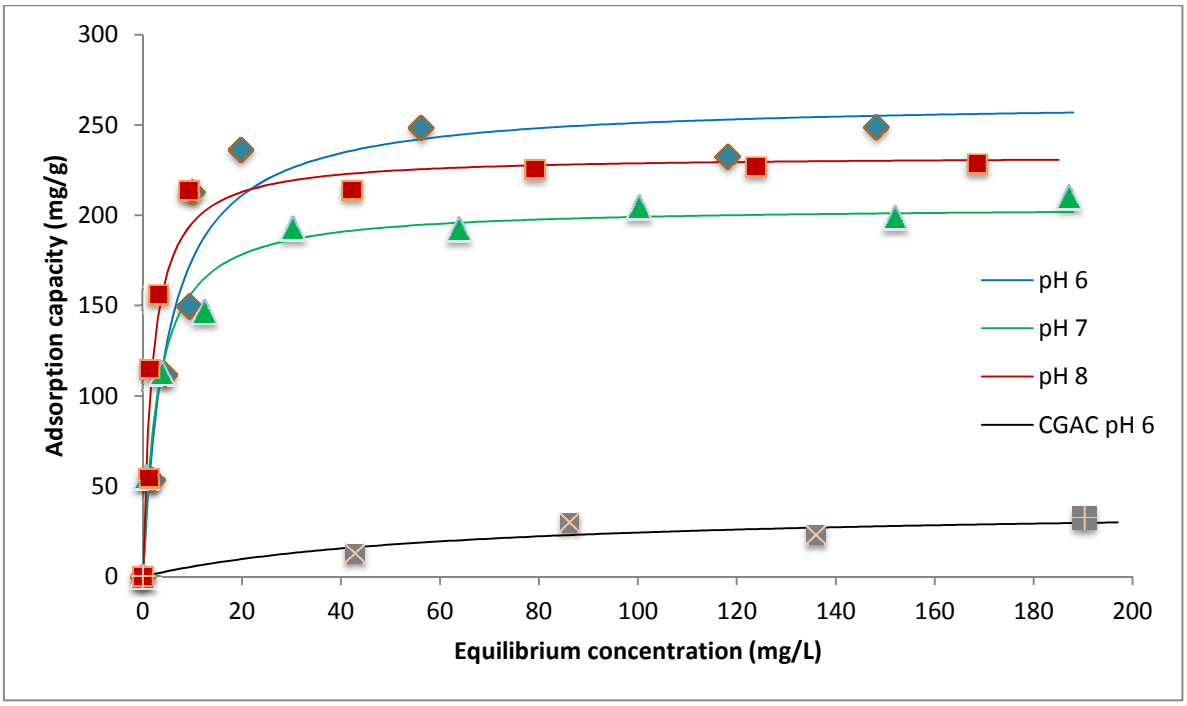

Figure 17 Chromate adsorption isotherms for DLH31500 at pH 6, 7 and 8 and activated carbon at pH 6.

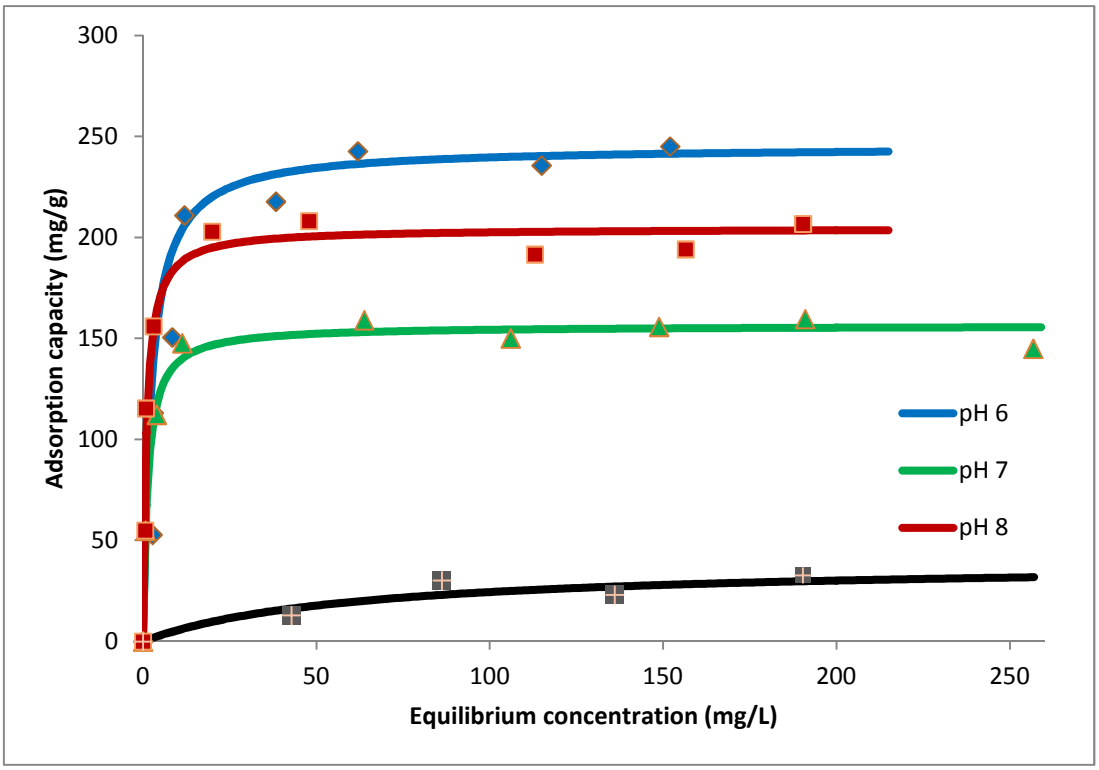

Figure 18 Chromate adsorption isotherms for DLH31600 at pH 6, 7 and 8 and activated carbon at pH 6.

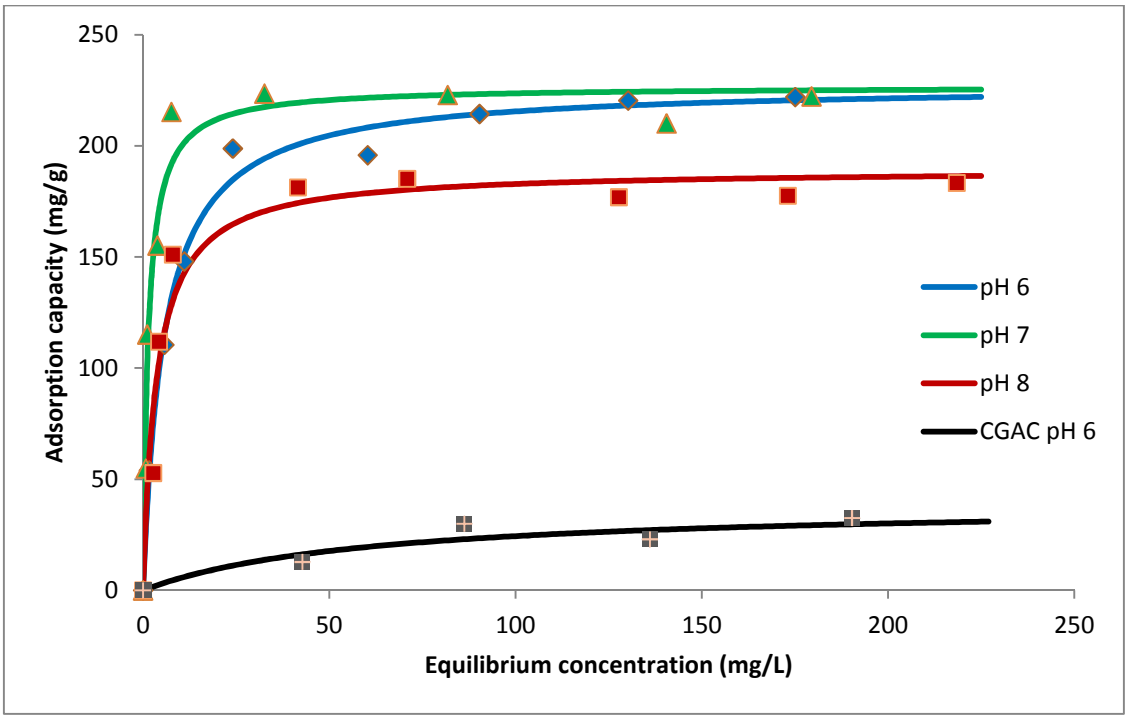

Figure 19 Chromate adsorption isotherms for DLHCL31500 at pH 6, 7 and 8 and activated carbon at pH 6.

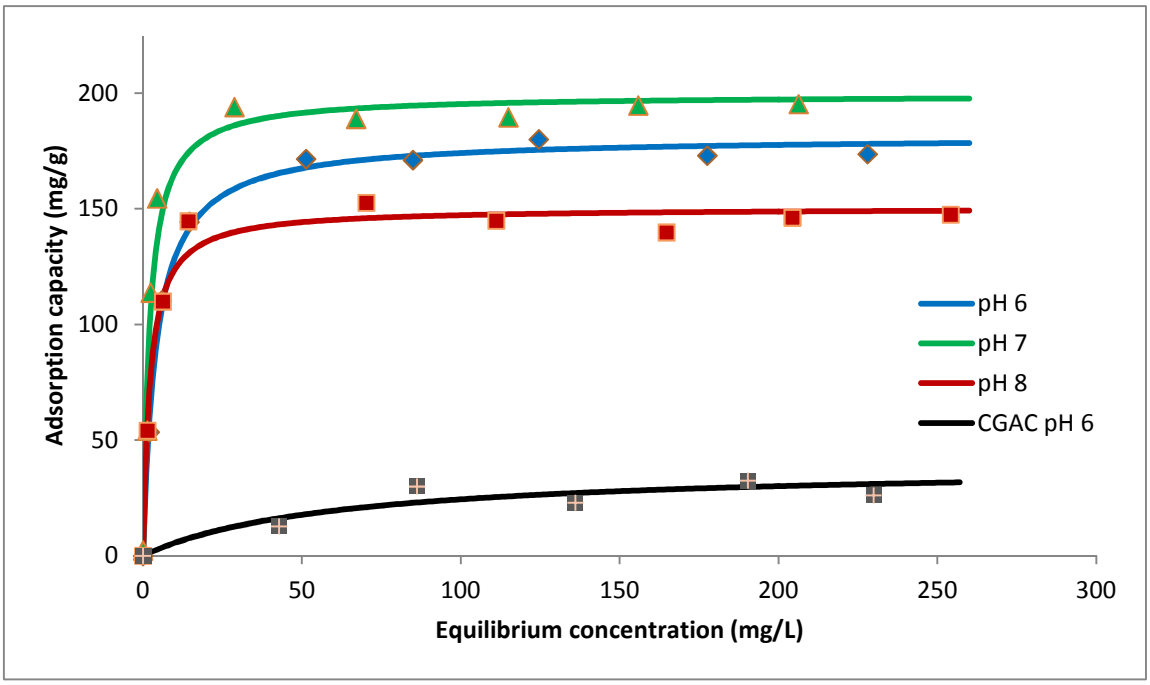

Figure 20 Chromate adsorption isotherms for DLHCL31600 at pH 6, 7 and 8 and activated carbon at pH 6.

Isotherms of Figures 7.11 to 7.14 shows that the best adsorbent and pH condition was the double-layered hydroxides with molar ratio of 3:1, with carbonate as exchange anion and thermal treatment temperature of 500 °C (HDL31500), and pH value of 6, showing an adsorption capacity of 248.91 mg/g at room temperature. With this result, DLH31500 adsorbent is going to be used at pH 6.

Table 9 Maximum adsorption capacities of chromate on the selected DLH adsorbents and CAGC at different pH values.

Adsorbent	pH	Adsorption capacity (mg/g)
DLH31500	**6**	248.91
	7	209.95
	8	228.47
DLH31600	**6**	245.08
	7	159.67
	8	206.76
DLHCL31500	**6**	222.00
	7	222.26
	8	183.30
DLH31CL600	**6**	173.72
	7	195.43
	8	147.53
CGAC	**6**	72.17
	7	32.99
	8	17.46

2.7 Bromate isotherms

Once that the best adsorbent was chosen, it was used to carry out bromate isotherms, kinetic and packed bed column test once that the equipment was available.

Figure 21 shows that the best pH condition to reach the highest adsorption capacity to remove bromate from water is pH 6; this is because when at pH 6 the concentration of hydroxyl ions is lower than at the other pH values (7 and 8), which resulted in less competition for bromate anions in adsorption sites. Also, the bromate isotherm of CAGC is shown for comparison; only the best pH is plotted. Maximum adsorption capacities are shown in Table 10.

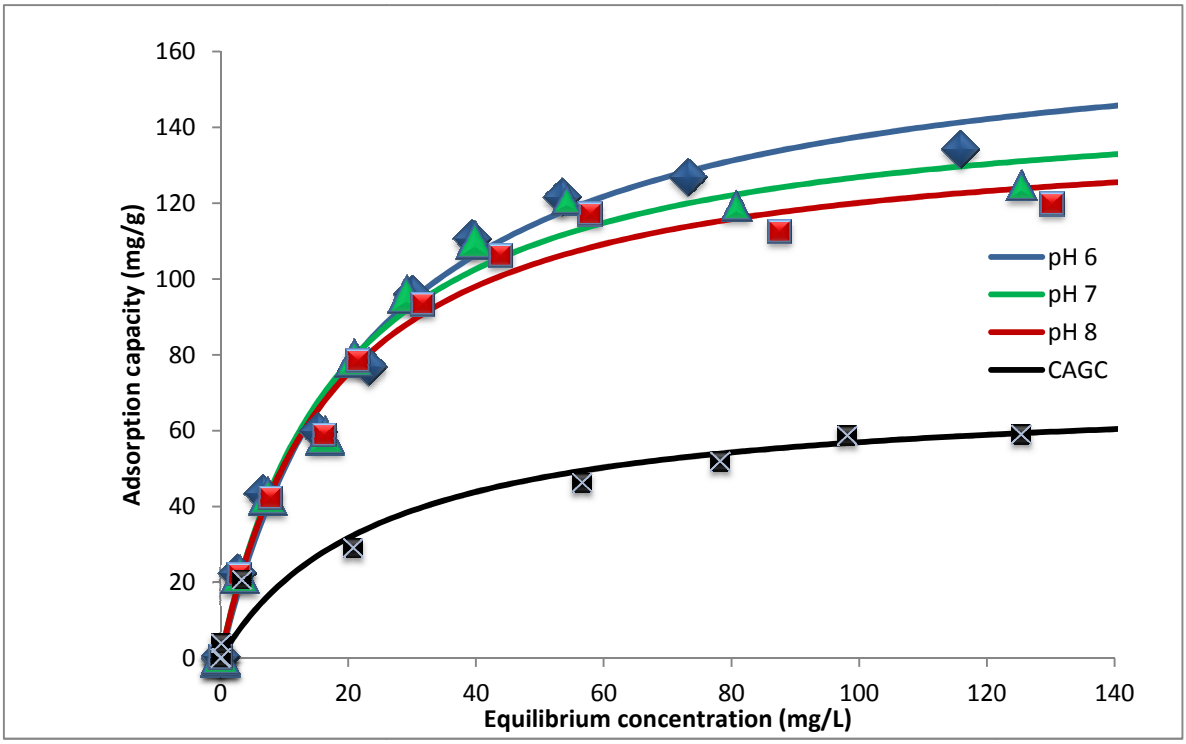

Figure 21 Bromate adsorption isotherms for selected double-layered hydroxides (DLH31500) at pH 6, 7 and 8 and activated carbon (CGAC) at pH 6.

Table 10 Maximum adsorption capacity of bromate on calcined DLH and activated carbon at different pH values.

Adsorbent	pH	Adsorption capacity (mg/g)
DLH31500	**6**	134.10
	7	124.52
	8	119.74
CGAC	**6**	66.07
	7	62.15
	8	60.18

Taking into account that DLH31500 had an adsorption capacity of 248.91 mg/g and 134.10 mg/g for chromate and bromate, respectively, (almost half of adsorption capacity); another adsorbent was tested to improve the bromate removal. Based on Liu *et al.* studies [60], a modified activated carbon was prepared by placing 20 g of activated carbon in 200 mL of 15% concentrated ammonia solutions and soaked for 24h. Then the modified carbon was washed with deionized water to neutral pH and dried at 105 °C for 24 h. Once that the new adsorbent was ready, isotherms for the modified activated carbon (MAC) were carried out at pH 6, 7 and 8.

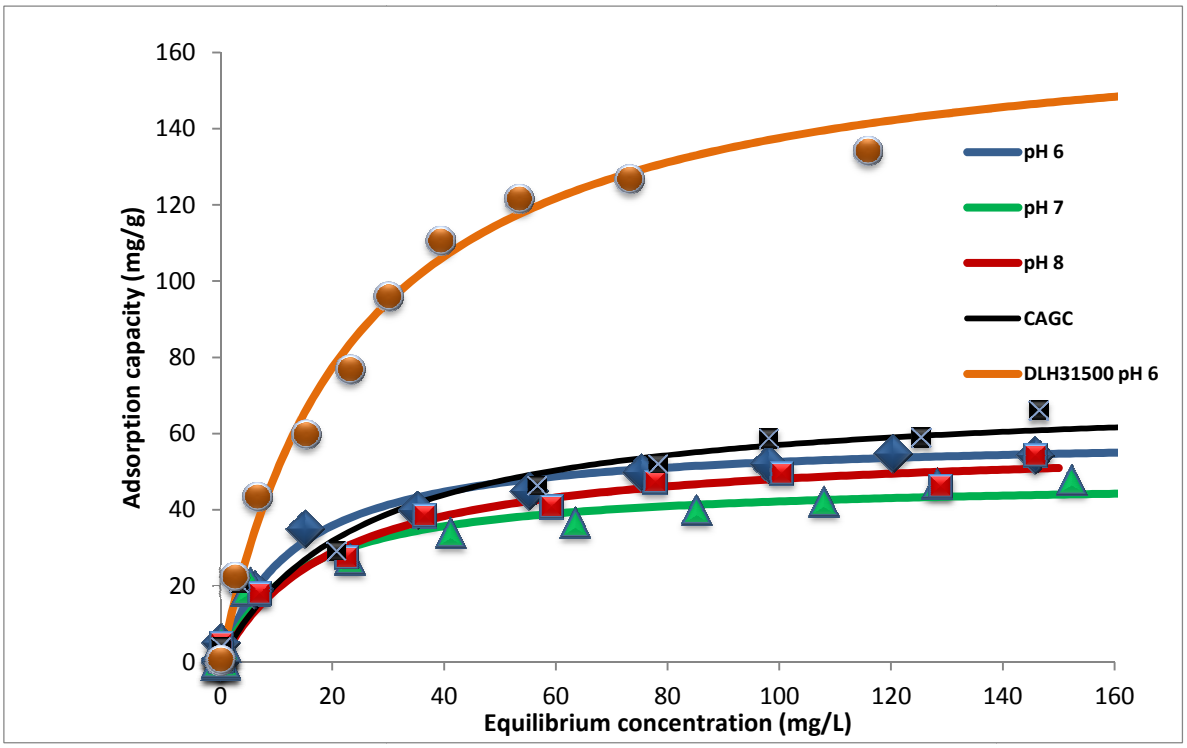

Figure 22 Modified activated carbon adsorption isotherms at pH 6, 7 and 8 for bromate removal.

Table 11 Maximum adsorption capacity of bromate onto raw (CGAC) and modified activated carbon (MAC) at pH 6, 7 and 8.

Adsorbent	pH	Adsorption capacity (mg/g)
MAC	**6**	54.52
	7	47.61
	8	54.14
CGAC	**6**	66.07
	7	62.15
	8	60.18

Even though activated carbon (66.07 mg/g) and modified activated carbon (54.52 mg/g) were used for bromate removal, DLH presented higher adsorption capacity (134.10 mg/g).

7.8 Chromate kinetic studies

Once the best adsorbent was selected and the maximum adsorption capacities were calculated, kinetic studies were performed at different mixing velocities (100, 200, 300 and 400 rpm) for chromate to calculate the kinetic parameters and adsorption capacity. The mixing system used for the kinetic studies is shown at Figure 6.

Table 12 Number, quantity, and time of the aliquots taken in kinetic studies.

Aliquot number	Aliquot quantity [mL]	Time [min]
1	1.0	0
2	1.0	1
3	1.0	3
4	1.0	5
5	1.0	7
6	1.0	10
7	1.0	15
8	1.0	20
9	1.0	30
10	1.0	45
11	1.0	60
12	1.0	90
13	1.0	120
14	1.0	150
15	1.0	200
16	1.0	250
17	1.0	300
18	1.0	420
19	1.0	540
20	1.0	700
21	1.0	1400
22	1.0	2000
23	1.0	2400

Determining the concentration of each aliquot was performed by colorimetric method coupled with UV-vis spectroscopy according to NMX-AA-044-SCFI-2001, with an initial chromate concentration of 200 mg/L.

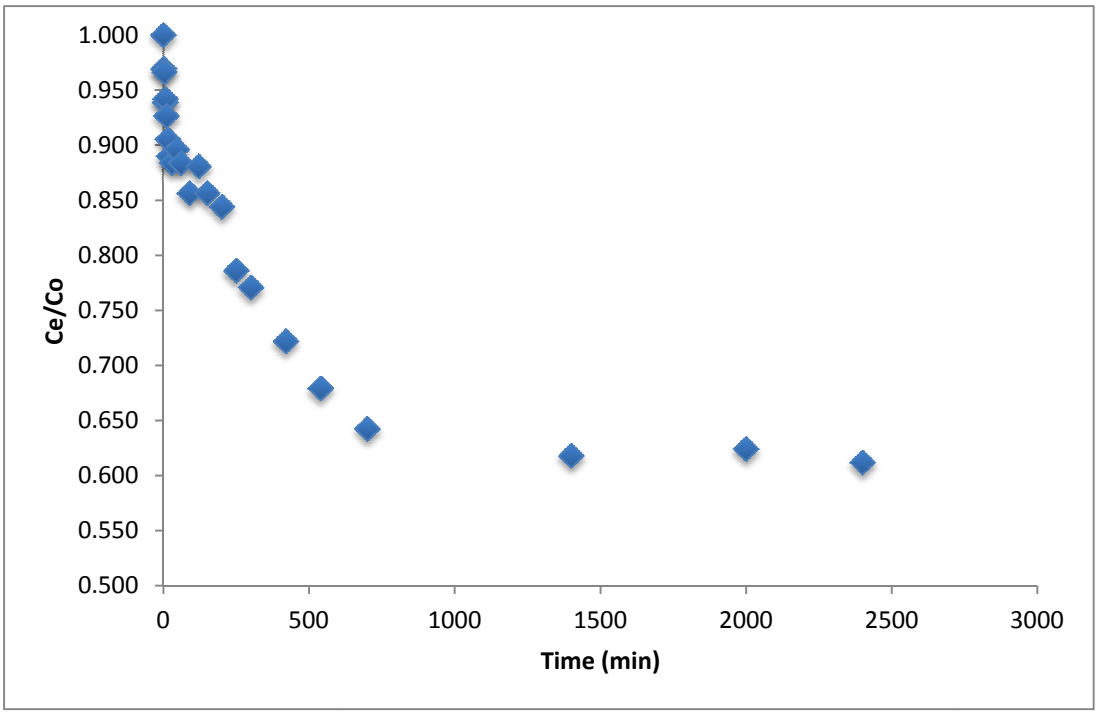

Figure 23 Adsorption kinetics of chromate onto DLH31500 at pH 6 at 100 rpm.

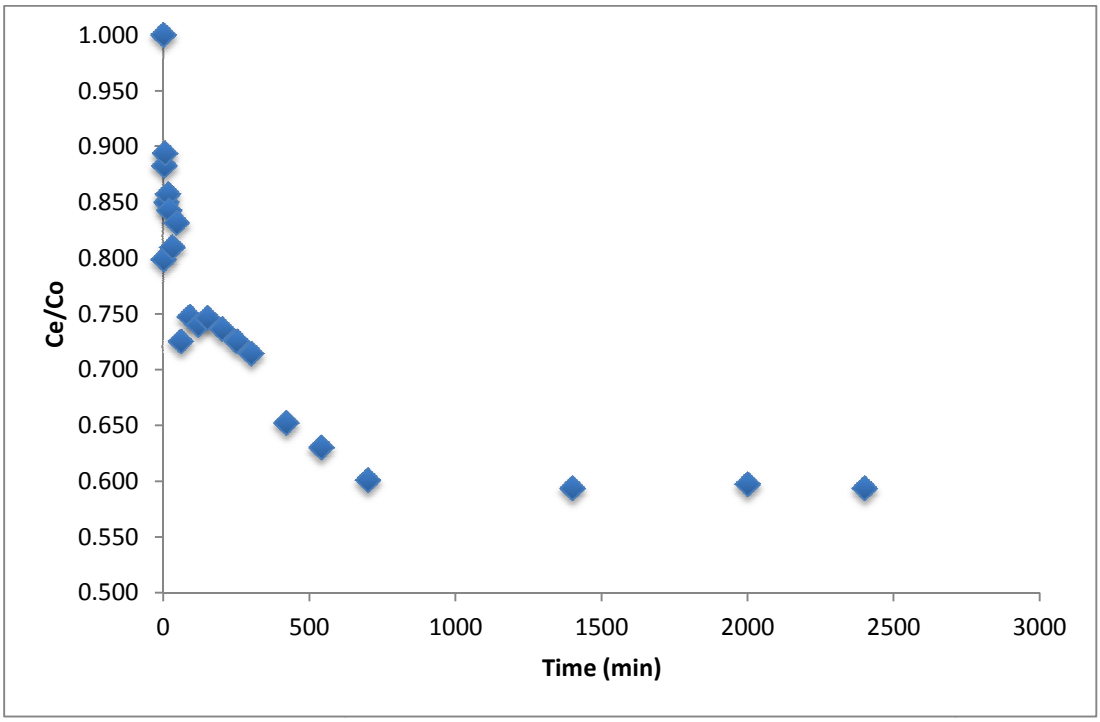

Figure 24 Adsorption kinetics of chromate onto DLH31500 at pH 6 at 200 rpm.

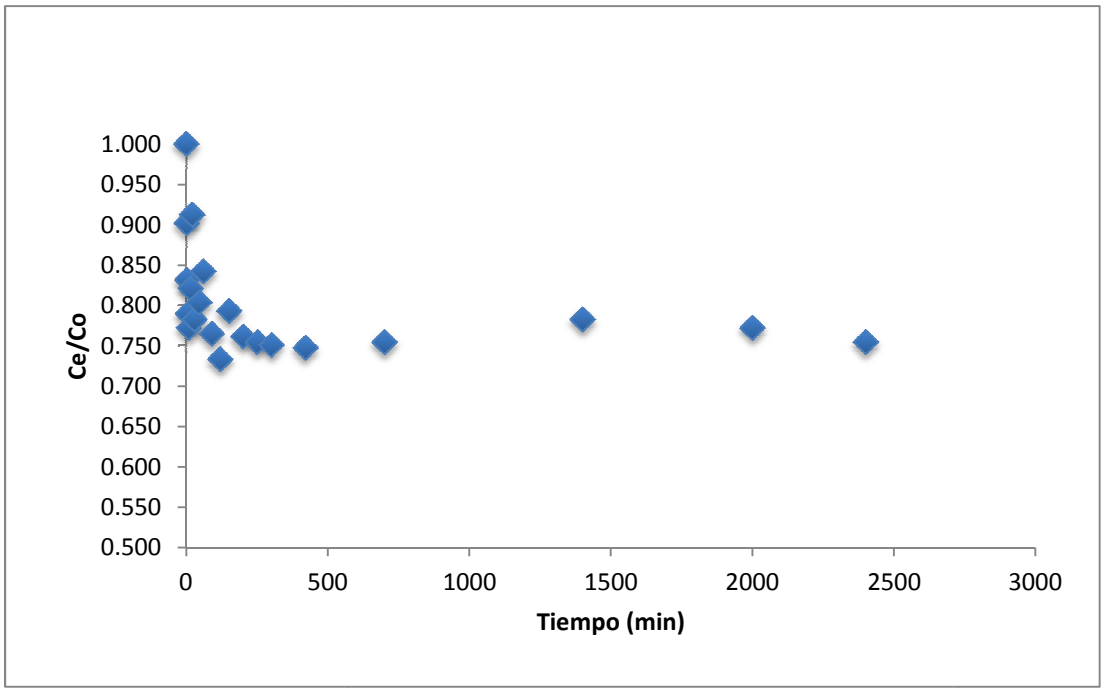

Figure 25 Adsorption kinetics of chromate onto DLH31500 at pH 6 at 300 rpm.

The kinetic study which present best adsorption capacities and Ce/Co values is the system with the lowest mixing velocity. It can be seen when the velocity is increased the adsorption capacity and the Ce/Co values decreased; this can happen because the anion in solution (with high mixing velocity) has enough energy to go out of the adsorption site [70], so the reformation of the structure will not occur and with this adsorption will not occur as well. Also as the mixing velocity is increase the more movement the solution has which leads to more air contact (carbonate presence) that can compete for the adsorption sites in the adsorbent. To confirm if a negative effect was caused by the presence of carbonate in the solution, kinetics with no-air presence (Argon atmosphere) were conducted. Sections 7.8 and 7.9 show kinetics with air and no air presence and a positive effect is observed when Argon was bubbled in the solution and then isolated. Likewise, for more information, XRD diffractograms were conducted for the lowest and highest mixing velocities. Figure 26 show the diffractogram for 100 rpm and 300 rpm, respectively.

Table 13 Values of chromate adsorption capacity (q_e) and C_e/C_o at 100, 200, and 300 rpm.

	100 rpm		200 rpm		300 rpm	
Time (min)	**Qe (mg/g)**	**Ce/Co**	**Qe (mg/g)**	**Ce/Co**	**Qe (mg/g)**	**Ce/Co**
0	0.000	1.000	0.001	1.000	0.000	1.000
1	7.984	0.969	43.910	0.799	22.354	0.902
3	8.782	0.966	25.548	0.883	38.321	0.832
5	15.967	0.939	23.153	0.894	47.901	0.789
10	19.161	0.927	32.733	0.850	51.893	0.772
15	24.749	0.905	31.137	0.857	40.716	0.821
20	28.741	0.890	34.330	0.842	19.959	0.912
30	30.338	0.884	41.515	0.810	49.498	0.782
45	27.144	0.896	36.725	0.831	44.708	0.804
60	30.338	0.884	59.877	0.725	35.926	0.842
90	37.523	0.856	55.087	0.747	53.489	0.765
120	31.136	0.881	56.684	0.740	60.675	0.733
150	37.523	0.856	98.996	0.546	47.103	0.793
200	40.716	0.844	57.482	0.736	54.288	0.761
250	55.885	0.786	59.877	0.725	55.884	0.754
300	59.877	0.771	62.272	0.714	56.683	0.751
420	72.650	0.722	75.844	0.652	57.481	0.747
540	83.827	0.679	80.634	0.630	227.529	0.000
700	93.407	0.642	87.021	0.601	55.884	0.754
1400	99.794	0.618	88.618	0.593	49.498	0.782
2000	98.197	0.624	87.819	0.597	51.893	0.772
2400	101.391	0.612	88.618	0.593	55.884	0.754

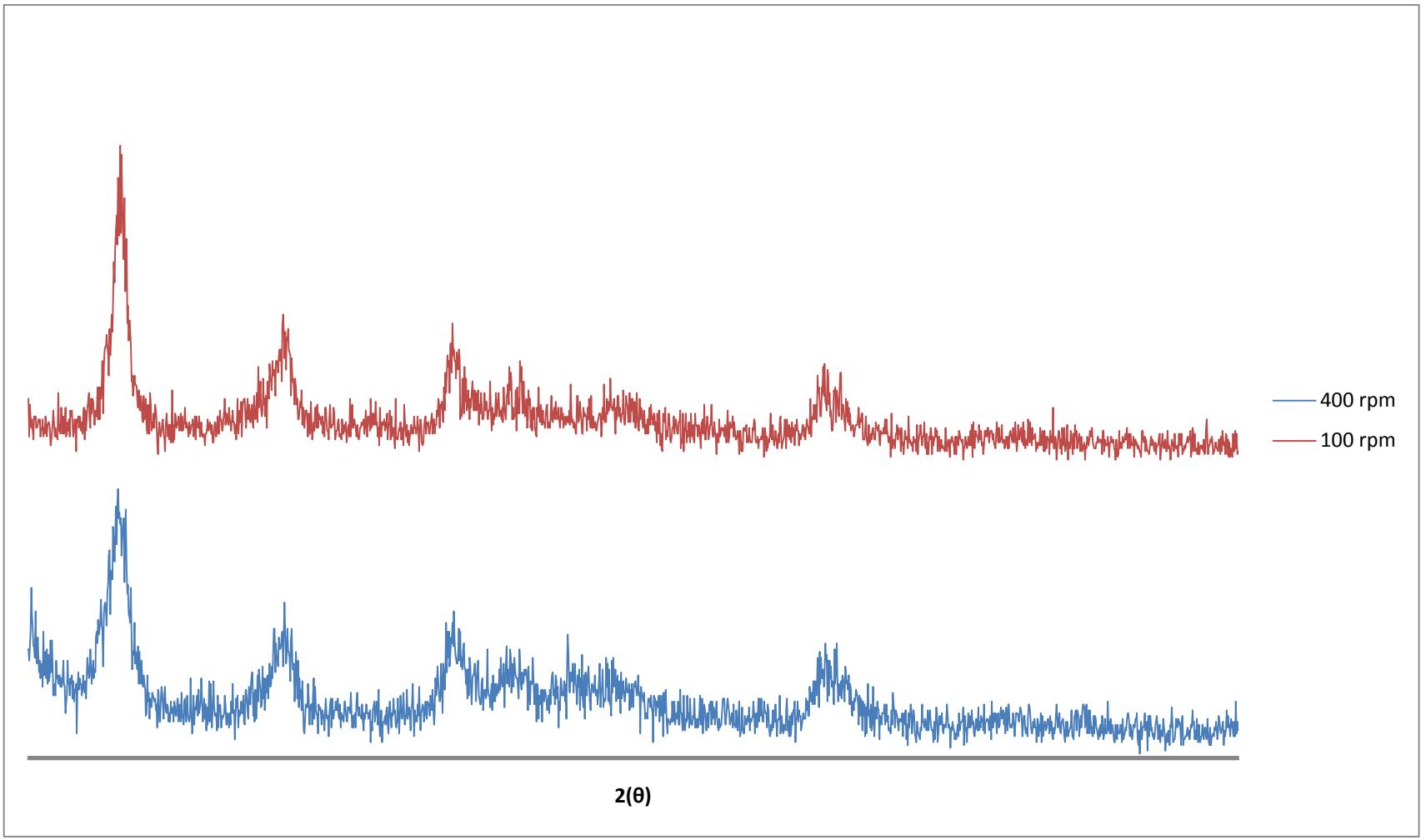

Figure 26 XRD diffractogram for DLH31500 at 100 and 400 rpm.

Figure 26 present less background noise which is attributed to the better formation and alignment of the double-layered hydroxides sheets, like in the synthesis, when slow mixing velocity (100 rpm) is needed in order to avoid breaking the sheets in the material [71].

But, even though the 100 rpm was the best mixing velocity of the mechanical system, it did not reach low Ce/Co values and the expected adsorption capacity values (169.38 mg/g for an initial concentration of 200 mg/L), so other systems were performed to prove if the system is a limiting factor.

The next systems were oscillatory, magnetic, and intermittent mixing. Figure 27 to 29 show the kinetic studies plots for HDL31500 for each of the systems in their lowest mixing velocity values.

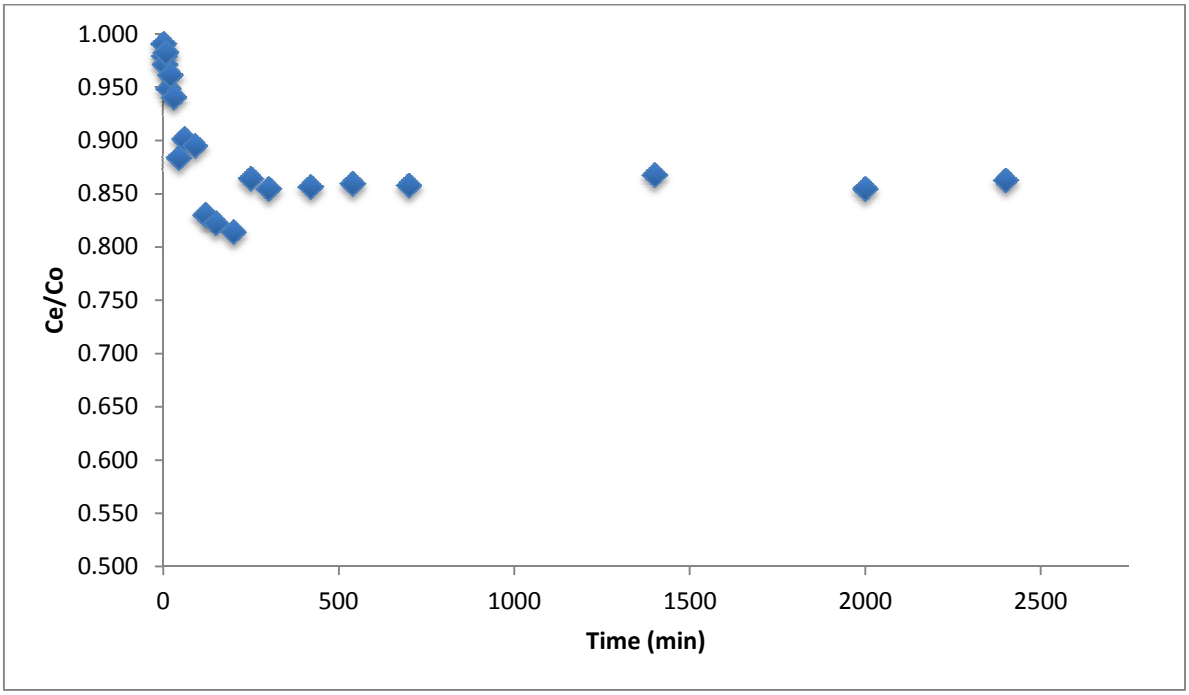

Figure 27 Adsorption kinetics of chromate on DLH31500 with magnetic-stirred system.

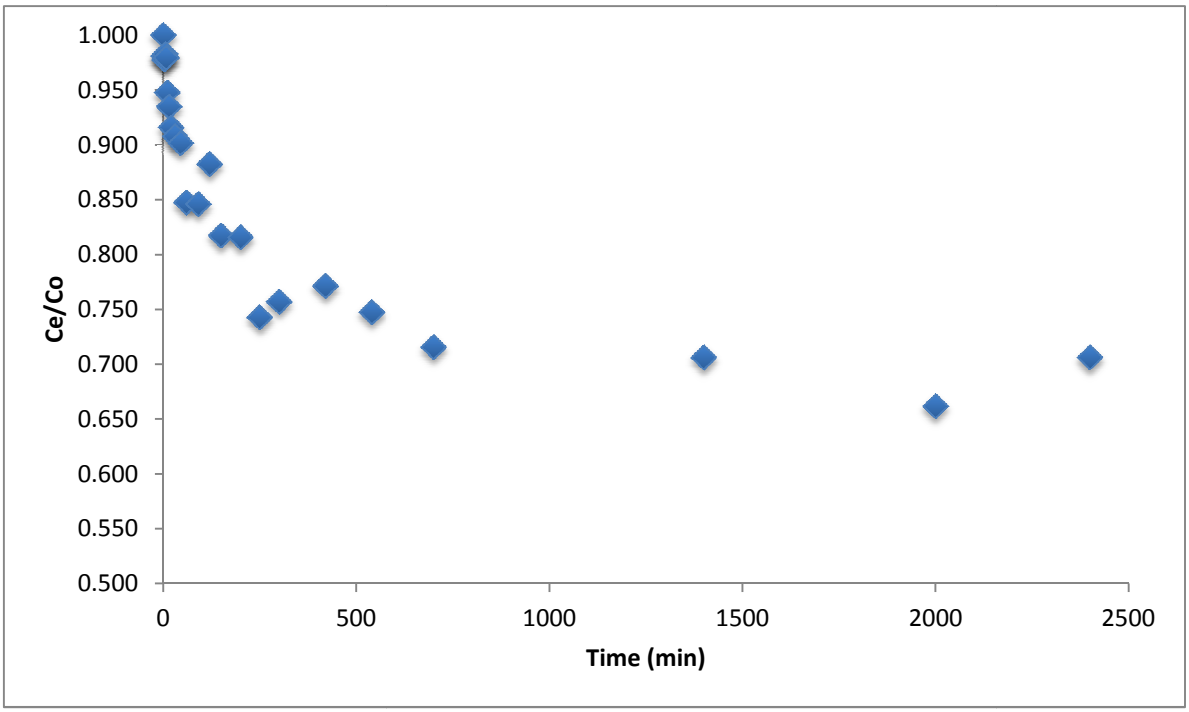

Figure 28 Adsorption kinetics of chromate on DLH31500 with oscillatory-stirred system.

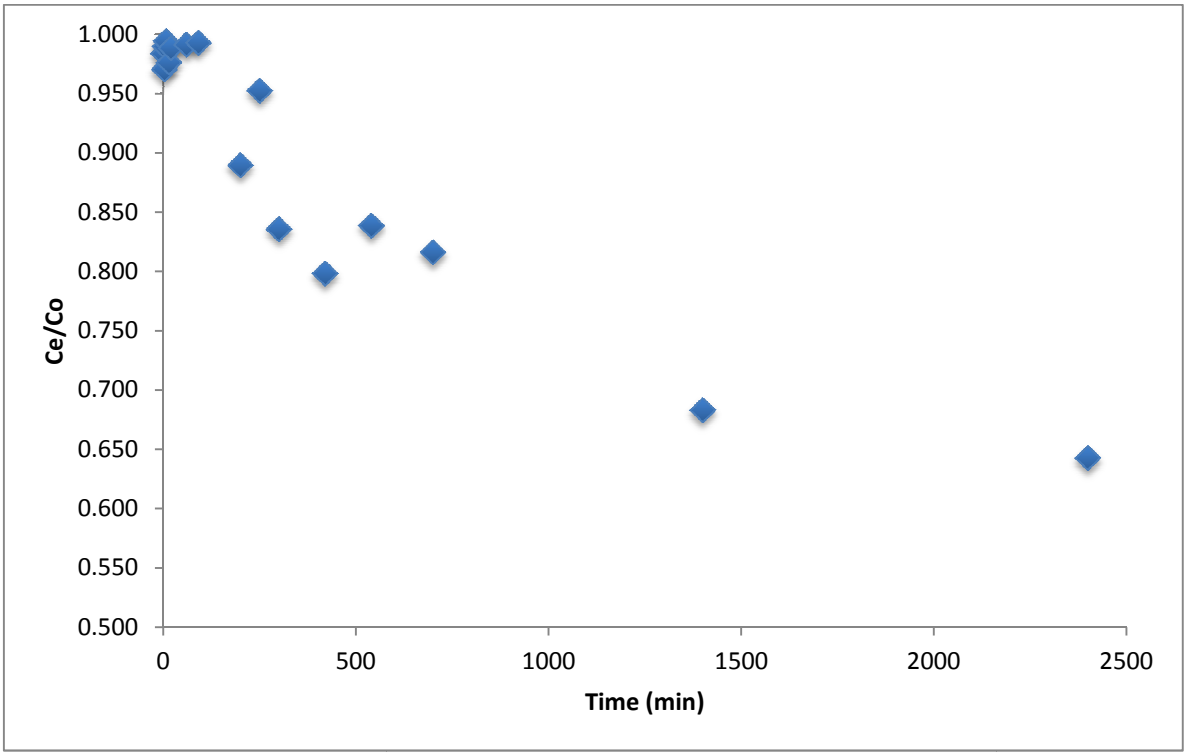

Figure 29 Adsorption kinetics of chromate on DLH31500 with intermittent-stirred system.

Table 14 Values of chromate adsorption capacity (q_e) and C_e/C_o for the oscillatory, magnetic, and intermittent mixing systems.

	Magnetic		Oscillatory		Intermittent	
Time [min]	**qe [mg/g]**	**Ce/Co**	**qe [mg/g]**	**Ce/Co**	**qe [mg/g]**	**Ce/Co**
0	0.000	1.000	0.000	1.000	0.000	1.000
1	2.064	0.990	4.130	0.981	3.785	0.984
3	4.473	0.979	4.818	0.978	6.882	0.970
5	6.194	0.971	3.786	0.983	2.409	0.990
7	3.785	0.982	4.474	0.979	NA	NA
10	0.000	1.000	11.356	0.948	1.376	0.994
15	11.011	0.948	14.109	0.935	0.000	1.000
20	8.258	0.961	18.238	0.916	5.506	0.976
30	12.732	0.940	19.959	0.908	2.753	0.988
45	24.776	0.883	21.335	0.901	0.000	1.000
60	20.991	0.901	33.035	0.847	0.000	1.000
90	22.367	0.895	33.379	0.846	2.064	0.991
120	36.132	0.830	25.465	0.882	1.720	0.993
150	37.852	0.822	39.574	0.817	0.000	1.000
200	39.573	0.814	39.918	0.816	0.000	1.000
250	28.905	0.864	55.747	0.742	25.464	0.889
300	30.970	0.854	52.650	0.757	11.011	0.952
420	68.479	0.677	49.553	0.771	37.852	0.835
540	29.938	0.859	54.715	0.747	46.455	0.798
700	30.282	0.857	61.597	0.715	37.164	0.838
1400	28.217	0.867	63.662	0.706	42.326	0.816
2000	30.970	0.854	73.297	0.661	72.952	0.683
2400	29.24949	0.862238	63.66166	0.705881	82.243	0.642

Even though other systems were used, they did not reach the expected values of adsorption capacity and Ce/Co, so a new system with no air presence was proposed to tell if the absorption of CO_2 from air is affecting the adsorption of the studied pollutants caused by adsorption sites competition. The used system consisted of a 1 L plastic bottle were 1 L of a 200 ppm chromate solution was placed and bubbled with Argon to displace the present carbonate and since Argon is heavier than air, it will remain in the surface so no air can interact with the solution; after that parafilm was used to isolate the system and take samples (1 mL) with a syringe of 1 mL (between every taken sample an extra parafilm sheet was added.)

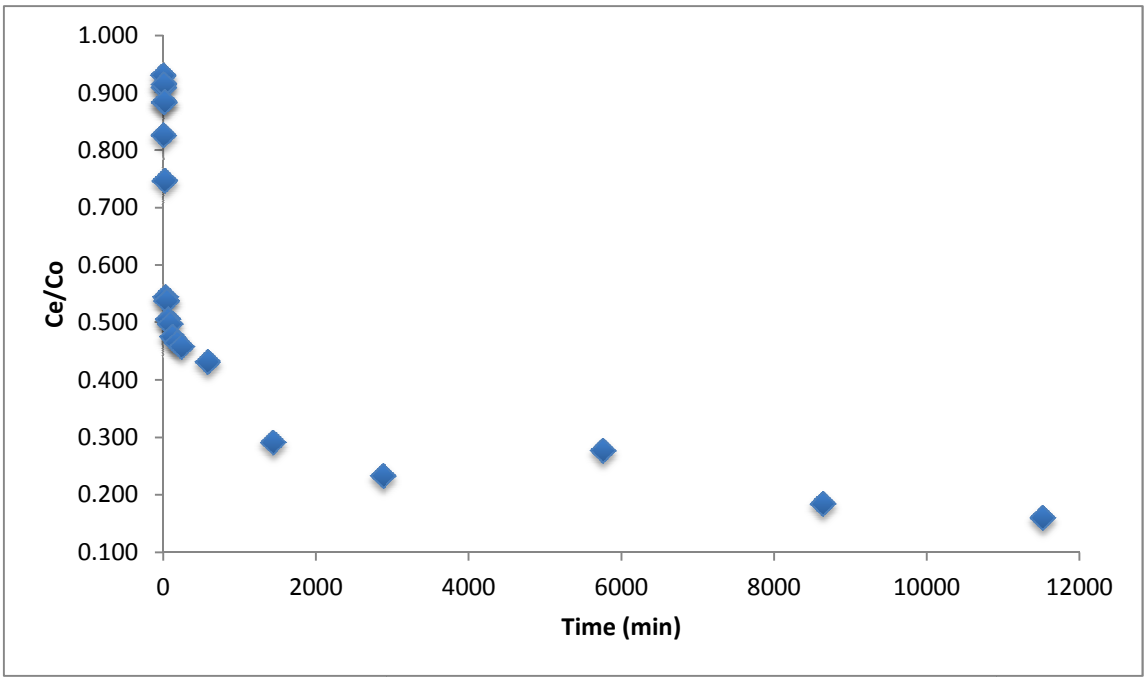

Figure 30 Adsorption kinetics of chromate on DLH31500 for no-air intermittent-stirred system.

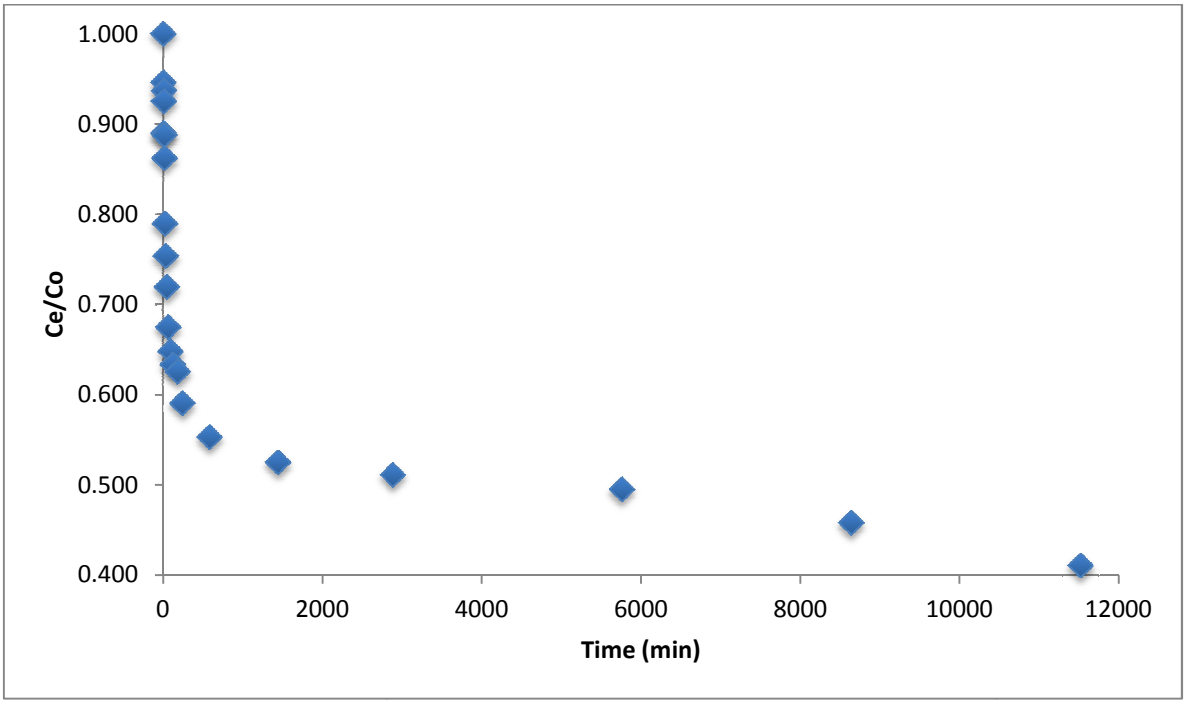

Figure 31 Bromate adsorption kinetics for DLH31500 for no-air intermittent-stirred system.

Table 15 Adsorption kinetics profile for chromate in the intermittent and no air presence.

Time [min]	qe [mg/g]	Ce/Co
0	0.000	1.000
1	14.025	0.930
3	34.948	0.826
5	18.234	0.909
7	17.139	0.915
10	23.472	0.883
15	23.282	0.884
20	50.815	0.747
30	91.424	0.544
45	92.805	0.537
60	99.210	0.505
90	100.829	0.497
120	105.234	0.475
180	107.377	0.464
240	108.782	0.457
580	114.067	0.431
1440	142.167	0.291
2880	153.889	0.232
5760	145.052	0.276
8640	163.609	0.184
11520	169.385	0.159

Using one of the first systems which could be set as a closed system (no air presence) with one of the best results was the intermittent mixing. The obtained results with the no-air and intermittent-stirred system were higher than those achieved with other systems previously proposed.

7.9 Bromate kinetic studies

For bromate kinetic, a system like chromate kinetic was used (1 L plastic bottle, bubbled with argon and isolated with parafilm). Samples of 2.5 mL were taken with a 5 mL syringe to determine bromate concentration by ion chromatography.

Table 16 Adsorption kinetics for bromate in the intermittent and no-air intermittent-stirred.

Tiempo	qe	Ce/Co
0	0.00	1.0000
1	19.79	0.8681
3	11.38	0.9241
5	16.74	0.8884
7	17.75	0.8817
10	25.79	0.8281
15	31.02	0.7932
20	33.77	0.7749
30	39.12	0.7392
45	47.64	0.6824
60	64.38	0.5708
90	57.59	0.6161
120	55.44	0.6304
180	59.77	0.6015
240	65.89	0.5607
580	89.89	0.4007
1440	85.00	0.4333
2880	95.13	0.3658
5760	103.00	0.3133
8640	102.00	0.3200
11600	110.38	0.2641

Bromate kinetic was performed obtaining that the equilibrium was reached at 5760 min approximately, and the maximum chromate adsorption capacity was 110.38 mg/g, bromate concentration decreased from 150.00 to 39.62 mg/L.

7.10 Packed bed column tests

In order to be able to carry out a continuous adsorption process a packed bed column was built using the selected adsorbent (DLH31500).

Different models were proposed and tested finding that using the same particle size (fine powder of DLH) as the batch tests developed backflow and leaking because there were not enough channels for the solution to flow through the adsorbent packed bed column. Hence, more adsorbent was synthesized in form of flakes (1.0 to 1.5 mm) to fill the column and create channels

so solution can fluid, even though the adsorption capacity will be reduce by increase the size particle (since the surface area is reduce), the solution could flow through the packed bed. The final system structure for the continuous adsorption tests is shown in Figure 34.

For chromate adsorption tests, 10 days and 15 min was the time until chromate was observed at the outlet and 13 days, 14 h and 40 min until the built column was saturated (Figure 32). This means that a total of 7.85 L of chromate solution were successfully treated (chromate concentration lower than 0.01 mg/L) having an adsorption capacity of 104.66 mg/g. The maximum adsorption capacity, calculated from the isotherm, was not reached probably due to the higher particle size used in this section (approximately 1 to 1.5 mm).

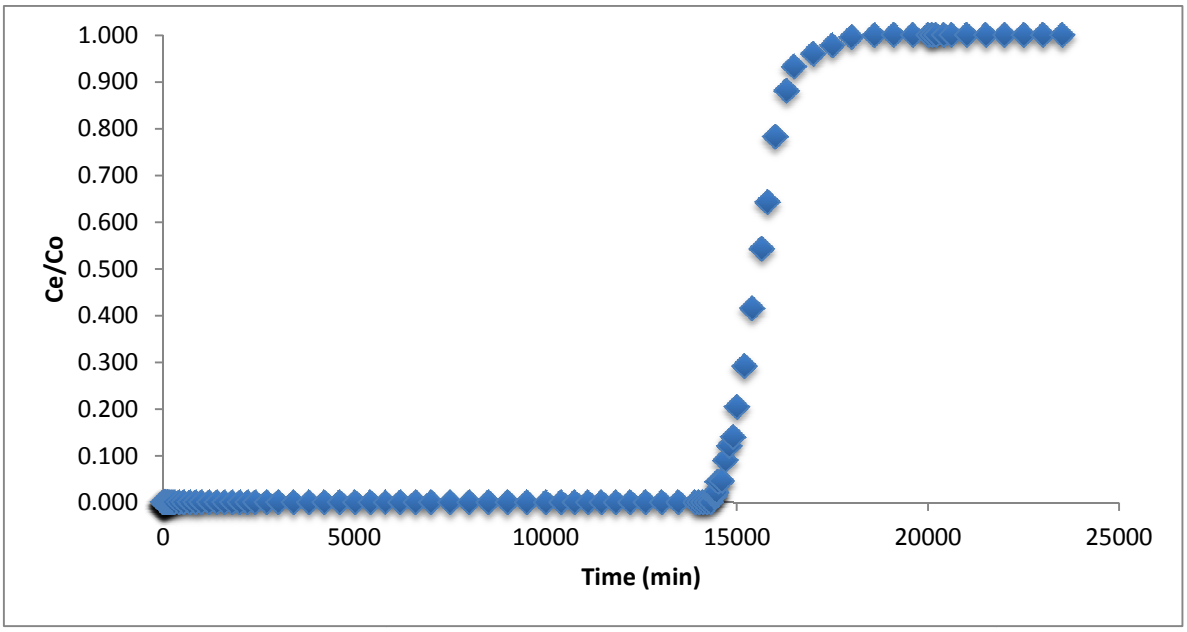

Figure 32 Packed bed column tests for chromate adsorption.

After 14 days 7 hours and 12 minutes bromate was observed at the outlet and 17 days, 16 hours and 37 minutes until the adsorption column was saturated. This results imply that a total of 13.73 L of bromate solution were successfully treated (bromate concentration lower than 0.01 mg/L) having an adsorption capacity of 45.77 mg/g. Because the higher particle size used (approximately 1 to 1.5 mm), the maximum adsorption capacity calculated from the bromate isotherm was not achieved, but it is a promising result.

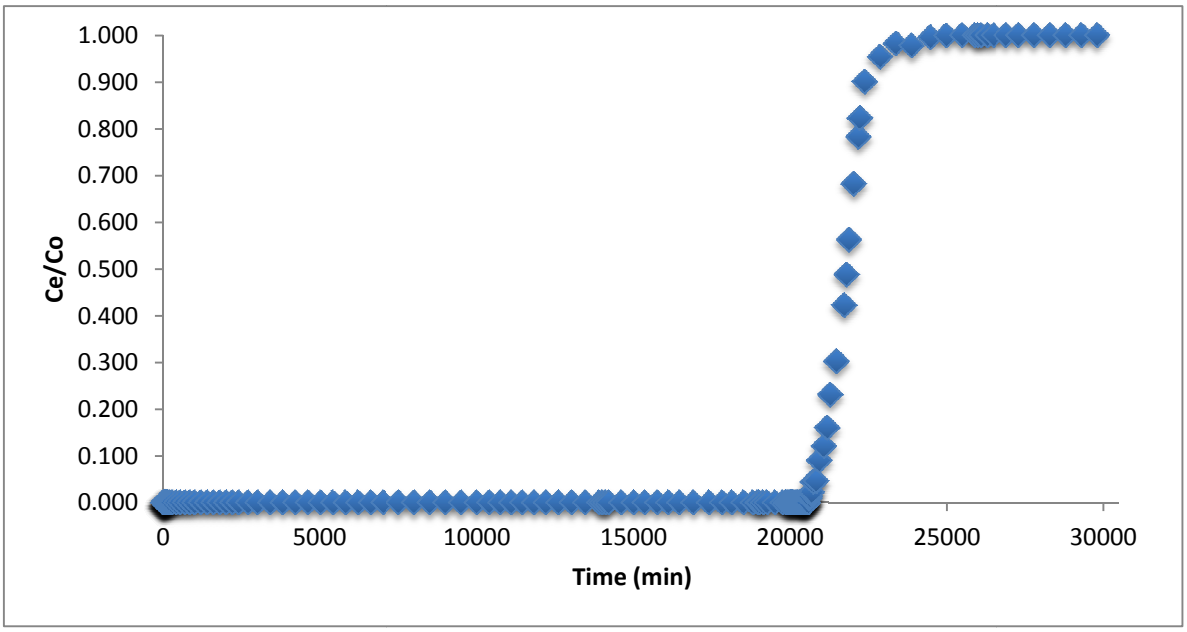

Figure 33 Packed bed column tests for bromate adsorption.

Double layered hydroxides presented a desorption capacity of 70.51 mg/g for chromate and 30.96 mg/g for bromate. After this, the adsorbent was calcined at 500 °C for 4 hours, and then it was replaced in the column reaching an adsorption capacity of 58.23 mg/g and 34.56 mg/g for chromate and bromate, respectively.

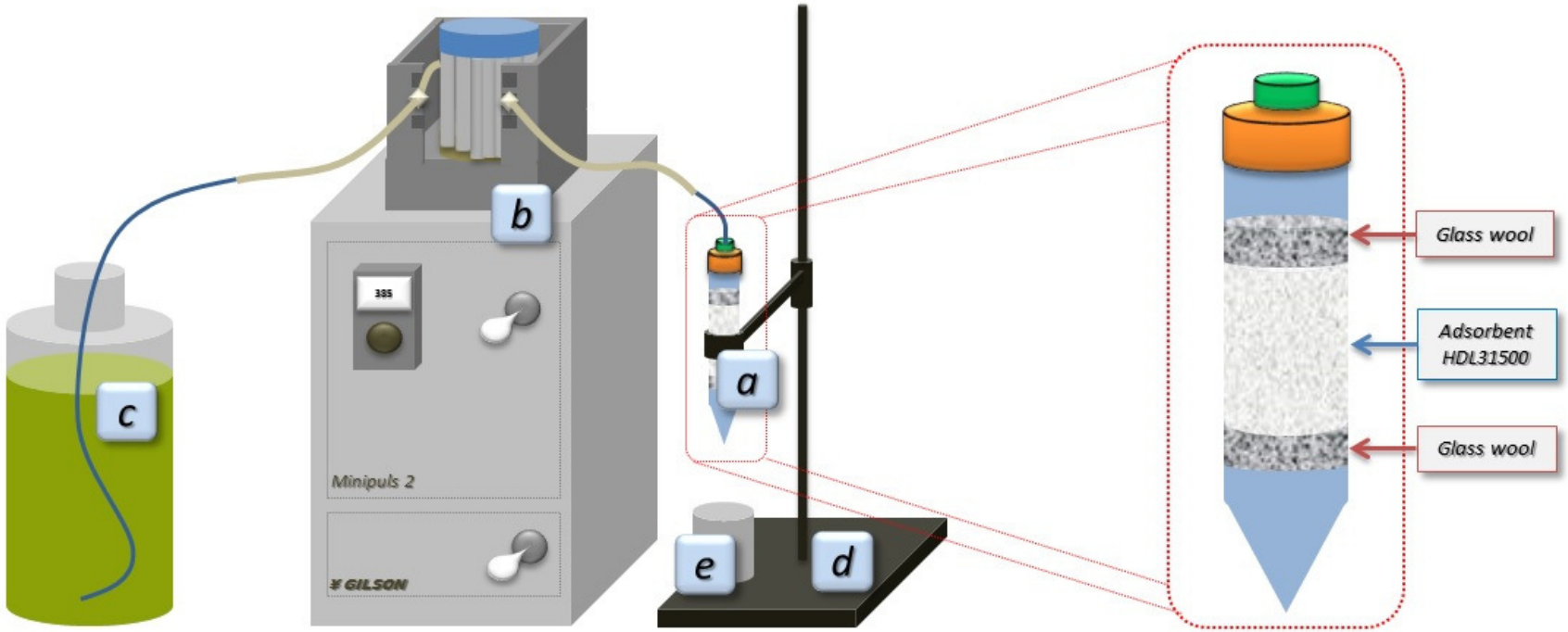

Figure 34 Packed bed column with DLH31500. A) Packed bed column (5 mL pipette tip), b) peristaltic pump (0.3 µL/min to 30 mL/min), c) 1 Liter plastic initial solution container, d) 60 cm metallic column holder, and e) 50 mL plastic final concentration container.

8 General conclusions

Mg-Al double-layered hydroxides have an adsorption capacity (248.91 mg/g for chromate and 134.1 mg/g for bromate) greater than commercial granular activated carbon (32.99 mg/g for chromate and 66.07 mg/g for bromate) and they can be used for bromate and chromate removal in aqueous solutions in batch and continuous process.

The synthesis of Mg-Al double-layered hydroxides by precipitation method was confirmed by characterization methods such as X ray powder diffraction with EVA™ database, thermogravimetric analysis, surface area analysis, scanning electron microscopy as well with the use of Bragg's equation for the calculation of interlayer space to confirm that each height correspond with the adsorbed anion size.

Double-layered hydroxides are clays with laminar structure that after calcination is destroyed, but once that the material is placed in a solution with anions such as bromate, chromate, etc., they present memory effect because the unraveled laminar structure is rebuilt. The reconstruction is possible because the anions present in the solution are attracted to the available positive sites in the sheets by electrostatic forces, so the higher the charge of an anion is, the stronger affinity they will have to the material; so this is the reason why double-layered hydroxide exhibited a higher adsorption capacity for chromate than for bromate in the adsorption/ desorption tests developed for all the synthesized materials.

Desorption tests of chromate and bromate-loaded double-layered hydroxides are conducted by using carbonate solution to regenerate the adsorbent as originally synthesized, been a good way to reuse the material accompanied with recalcination to disassemble again the laminar structure.

Adsorption isotherms show that Langmuir isotherm fit well to predict the adsorption behavior presenting high adsorption capacities (248.91 mg/g for chromate and 134.1 mg/g for bromate) in comparison with commercial activated carbon (32.99 mg/g for chromate and 66.07 mg/g for bromate) and the ammonia modified activated carbon for the removal of bromate (54.52 mg/g).

Furthermore, since the double-layered hydroxides have low porosity, low surface area and low pore volume, the adsorption is limited by an external mass transfer resistance and the reassembling stage.

Also, double-layered hydroxides can be used in continuous processes to treat water in real effluents with a particle size from 1 to 1.5 mm approximately, so the material can stay in the packed bed column with glass wool as support presenting a chromate adsorption capacity of 104.66 mg/g and a bromate adsorption capacity of 45.77 mg/g. Likewise, desorption tests is a required step to reuse the material for posterior adsorption tests showing desorption capacities for chromate and bromate of 70.51 mg/g and 30.96 mg/g, respectively.

Finally, adsorption of bromate and chromate by Mg-Al double-layered hydroxides is a promising way for the treatment of drinking water and wastewaters from diverse industries such as metal plating, leather tannery, textile, and metal finishing, among others. In addition, this adsorbent has a greater adsorption capacity than commercial activated carbons.

9 References

[1] Martínez, D., Carbajal, G., "Hidroxidos dobles laminares: arcillas sintéticas con aplicación en nanotecnología," *Avances en Química,* vol. 7 (1), pp. 87-99, 2012.

[2] Arakcheeva, A. V.; Pushcharovsky, D. Y., "Crystal structure and comparative crystal chemistry of Al2Mg4(OH)12(CO3)*3H2O, a new mineral from the hydrotalcite-manasseite group Note polytype 2H locality," *Crystallography Reports,* vol. 41, pp. 972-981, 1996.

[3] Russell, D., Shiang, D., "Thinking about more sustainable products: Using an efficient tool for sustainability education, innovation, and project managment to encourage sustainability thinking in a multinational corporation," *ACS Sustainable Chemical Engineering,* vol. 1, pp. 2-7, 2013.

[4] Enviromental Protection Agency, "Basic information about disinfection byproducts in drinking water: Total trihalomethanes, haloacetic acids, bromate, and chlorite," 13 December 2013. [Online]. Available: http://water.epa.gov/drink/contaminants/basicinformation/disinfectionbyproducts.cfm. [Accessed 27 December 2013].

[5] EPA, "Ozone, Alternative Disinfectants and Oxidants," Enviromental Protection Agency, 2002.

[6] Liu, C., Gunten, U., Croué, J.P., "Enhanced bromate formation during chlorination of bromide-containing waters in the presence of CuO," *Environmental Science & Technology,* vol. 46, pp. 11054-11061, 2012.

[7] Dong, W., Dong, Z., Zhu, R., Dong, Y., Ouyang, F., "Removal of Bromate from Water by Silver-Supported Activated Carbon.," *Energy and Enviromental Technology,* vol. 2, pp. 687-690, 2009.

[8] Synder, A., Vanderford, J., Rexing, J., "Trace Analysis of Bromate, Chlorate, Iodate and Perchlorate in Natural Bottled Waters.," *Environmental Science & Technology,* vol. 39, p. 4586 – 4593, 2005.

[9] World Health Organization, "WHO Guidelines for drinking-water quality," WHO, 2005.

[10] Leyva, R., Flores, J., Díaz, P., Berber, M., "Adsorción de Cromo (VI) en solución acuosa sobre fibra de carbon activado," *Información Tecnológica,* vol. 19 (5), pp. 27-36, 2008.

[11] Kuo, S., Bembeneck, R., "Sorption and desorption of chromate by wood shavings impregnated with iron or aluminum oxide," *Bioresource Technology ,* vol. 99, pp. 5617-5625, 2008.

[12] John C. Crittenden, R. Rhodes Trussell, David W. H, Water Treatment: Principles and Design, Hoboken, New Jersey: John Wiley & Sons, Inc., 2012.

[13] Haydar, S., Azziz, J., "Coagulation–flocculation studies of tannery wastewater using combination of alum with cationic and anionic polymers," *Journal of Hazardous Materials,* vol. 168, no. 2-3, p. 1035–1040, 2009.

[14] Listiarini, K., Tor, J., Sun, D., "Hybrid coagulation–nanofiltration membrane for removal of bromate and humic acid in water," *Journal of Membrane Science,* vol. 365, no. 1-2, p. 154–159, 2010.

[15] Rengaraj, S., Yeon, K., Moon, S.H., "Removal of chromium from water and wastewater by ion exchange resins," *Journal of Hazardous Materials,* vol. 87, no. 1-3, p. 273–287, 2001.

[16] Matos, C., Velizarov, S., Reis, M., "Removal of bromate from drinking water using the ion exchange membrane bioreactor concept," *Environmental Science and Technology,* vol. 42, pp. 7702-7708, 2008.

[17] Gyparakis, S., Diamodópoulus, E., "Formation and reverse osmosis removal of bromate ions during ozonation of groundwater in coastal areas," *Separation Science and Technology,* vol. 42, pp. 1465-1476, 2007.

[18] Mohan, D., Pittman, C., "Activated carbons and low cost adsorbents for remediation of tri- and hexavalent chromium from water," *Journal of Hazardous Materials,* vol. B137, pp. 762-811, 2006.

[19] Sánchez-Polo, M., Rivera-Utrilla, J., Salhi, E., "Removal of bromide and iodide anions from drinking water by silver-activated carbon," *Journal of Colloid and Interface Science,* vol. 300, pp. 437-441, 2006.

[20] Metcalf and Eddy, "Waste Water Engineering Treatment and Reuse," in *Advanced Waste Water Treatment*, McGraw Hill USA, 2004, p. 1113 – 1161.

[21] Bottani, E., Tascón, J.M., "Overview of physical adsorption by carbond," in *Adsorption by Carbons*, Elsevier, 2003, pp. 3-12.

[22] Mangun, C., Benak, K., Economy, J., Foster, K., "Surface chemistry, pore size and adsorption properties of activated carbon fibers and precursos treated with ammonia," *Carbon,* vol. 39, pp. 1809-1820, 2001.

[23] Fang, J., Gu, Z., Gang, D., Liu, C., Ilton, E., "Cr(VI) Removal from aqueous solution by activated carbon coated with quaternized poly(4-vinylpyridine)," *Environmental Science and Technology,* vol. 41, pp. 4748-4753, 2007.

[24] Dakiki, M., Khamis, M., Manassra, A., Mer'eb, M., "Selective adsorption of chromium(VI) in industrial wastewater using low-cost abundantly available adsorbents," *Advances in Environmental Research,* vol. 6, no. 4, pp. 533-540, 2002.

[25] Mor, S., Ravindra, K., Bishnoi, N., "Adsorption of chromium from aqueous solution by activated alumina and activated charcoal," *Chemical Engineering Journal,* vol. 10, pp. 261-268, 1996.

[26] Leyva-Ramos, R., Rangel-Mendez, J.R., "Intraparticle diffusion of cadmium and zinc ions during adsorption from aqueous solution on activated carbon," *Journal of Chemical Technology and Biotechnology,* vol. 80(8), pp. 924-933, 2005.

[27] Nondek, L., Frei, R.W., Brinkman U. A. Th., "Heterogenous catalytic post-column reaction detectors for high performance liquid chromatography application to n-methylcarbamates," *Journal of Chromatography A,* vol. 2282, pp. 141-150, 1983.

[28] Bajpai, A., Rajpoot, M., "Adsorption Techniques - A review," *Journal of Scientific and Industrial Research,* vol. 58, pp. 844-860, 1999.

[29] Cortés J.C., Giraldo, L., García, A., "Oxidación de un carbón activado comercial y sus caracterización del contenido de grupos ácidos superficiales," *Revista Colombiana de Química ,* vol. 37, no. 1, pp. 55-65, 2008.

[30] Bagreev, A., Menendez, J.A., Duckhno I., "Bituminous coal based activated carbon modified with nitrogen as adsorbents of hydrogen sulfide," *Carbon,* vol. 42, pp. 469-476, 2004.

[31] Quintana, C., Roque P., González G., "Ash content on activated carbons," *Centro Azúcar,* vol. 17, pp. 77-80, 1990.

[32] Barret, E., Joyner L., Halenda P., "The Determination of Pore Volume and Area Distributions in Porous Substances. I. Computations from Nitrogen Isotherms," *Journal of American Chemical Society,* vol. 73, no. 1, p. 373–380, 1951.

[33] Boyd, G.E., Schubert J., Adamson W., "The exchange adsorption of ions from aqueous solutions by organic zeolites. I. Ion-exchange equilibria," *Journal of American Chemical Society,* vol. 69, no. 11, pp. 2818-2829, 1947.

[34] Aguado, S., Polo, A., Bernal, M., Coronas, J., "Removal of pollutants from indoor air using zeolite membranes," *J. of Membrane Science,* vol. 240, no. 1-2, pp. 159-166, 2004.

[35] Vermeiren, W., Gilson, J.P., "Impact of zeolites on petroleum and Petrochemistry," *Topics in Catalysis,* vol. 52, pp. 1131-1161, 2009.

[36] Barthomeuf, D., "Basic zeolites: characterization and uses in adsorption and catalysis," *Catalysis Reviews: Science and Engineering,* pp. 125-149, 1996.

[37] Chen, Y., Kang, Y., Zhang, J., "New mimic of zeolite: heterometallic organic host framework accommodating inorganic cations," *Chemical Communications,* vol. 46(18), pp. 3182-3184, 2010.

[38] Ajayan, P., Stephan, O., Colliex,C., Trauth, D. , "Aligned carbon nanotube arrays formed by cutting a polymer resin-nanotube composite," *Science,* vol. 256, pp. 1212-1214, 1994.

[39] Müller, E., "Comparison between mass transfer properties of weak-anion-exchange resins with graft-functionalized polymer layers and traditional ungrafted resins," *Journal of Chromatography A,* vol. 1006, no. 1-2, pp. 229-240, 2003.

[40] Martins, C., Ruggeri, G., De Paoli, M., "Synthesis in pilot plant scale ad physical properties of sulfonated polyestyrene," *Journal of Brazilian Chemical Society,* vol. 14 (5), pp. 130-138, 2003.

[41] Wang. J., Chen, C., "Biosorbents for heavy metals removal and their future," *Biotechnology Advances,* vol. 27, no. 2, pp. 195-226, 2009.

[42] Strandberg, G., Shumate S., Parrott, J., "Microbial cells as biosorbents for heavy metals: Accumulation of uranium by Saccharomyces cerevisiae and Pseudonomas aerinosa," *Applied and Environmental Microbiology,* vol. 41(1), pp. 237-245, 2008.

[43] Wheeler, P., Wang, J., Baker J., Mathias, L., "Synthesis and characterization of covalently functionalized Laponite clay," *Chemistry of materials,* vol. 17(11), pp. 3012-3018, 2005.

[44] Luo, J.J., Daniel, I., "Characterization and modeling of mechanical behavior of polymer/clay nanocomposites," *Composites Science and Technology,* vol. 63, no. 11, pp. 1607-1616, 2003.

[45] C. C. P. V. C. C. C. Aguzzi, "Use of clays as drug delivery system: Possibilities and limitants," *Applied Clay Science,* vol. 36, no. 1-3, pp. 22-36, 2007.

[46] Chitrakar R., Sonoda, A., Makita Y., Hirotsu, T., "Calcined Mg-Al double layered hydroxides for uptake of trace levels of bromate from aqueous solutions," *Industrial Engineering Chemistry Research,* vol. 50, pp. 9280-9285, 2011.

[47] Chitrakar, R., Makita, Y., Sonoda, A., Hirotsu, T., "Fe–Al layered double hydroxides in bromate reduction: Synthesis and reactivity," *Journal of Colloid and Interface Science,* vol. 354, pp. 798-803, 2011.

[48] Newman, S., Jones, W. , "Synthesis, characterization and applications of layered double hydroxides containing organic guests," *New Journal of chemistry,* vol. 22, pp. 105-115, 1998.

[49] López-Salinas, E., Llanos-Serrano, M., "Characterization of synthetic hydrocalumite: Effect of the calcination temperature," *Journal of Porous Materials,* vol. 2, pp. 291-297, 1996.

[50] Purushothaman, M., Pugazthenthi, G., "Utilization of calcined Ni-Al layered double hydroxides (LDH) as an adsorbent for removal of methyl orange dye from aqueous solutions," *Enviromental Progress & Sustainable Energy,* vol. 33(1), pp. 154-159, 2013.

[51] Liang, L., Wang, Y., Wei, M., Cheng, J., "Bromide ion removal from contaminated water by calcined and uncalcined MgAl-CO3 layered double hydroxides," *Journal of Hazardous Materials ,* vol. 152, pp. 1130-1137, 2008.

[52] Liu, Z., Ma, R., Osada, M., Lyi, N., Ebina, Y., "Synthesis, anion exchange, and delamination of Co-Al layered double hydroxides: Assembly of the exfoliated nanosheet/polyanion composite films and magneto-optical studies," *Journal of the American Chemical Society,* vol. 128 (14), pp. 4872-4880, 2006.

[53] Crepaldi, E., Pavan, P., Valim, J., "Anion exchange in layered double hyroxides by sulfactant salt formation," *Journal of Materials Chemistry,* vol. 10, pp. 1337-1343, 2000.

[54] Constantino, V., Pinnavaia, T., "Basic porperties of Mg2+1-xAl3+x layered double hydroxide intercalated by carbonate, hydroxide, chloride, and sulfate anion," *Inorganic Chemistry,* vol. 34 (4), pp. 883-892, 1995.

[55] Rocha, J., del Arco, M., Rives, V., Ulibarri, M., "Reconstruction of layered double hydroxides from calcined precursors: a powder XRD and AL MAS NMR study," *Journal of Materials Chemistry,* vol. 9, pp. 2499-2503, 1999.

[56] Sugimoto, A., Ishida, S., Hanawa, K., "Preparation and characterization of Ni/Al layered double hydroxides," *Journal of the Electrochemical Society,* vol. 146, pp. 1251-1255, 1999.

[57] Reddy, R., Reddy, R., "Synthesis and electrochemical characterization of amorphous manganese oxide electrochemical capacitor electrode material," *Journal of Power Sources,* vol. 132, no. 1-2, pp. 135-320, 2004.

[58] Lametschwandtner, A., Lametschwandtner, A., "Scanning electron microscopy of vascular corrosion casts, technique and applications: updated review," *Europe PubMed Central,* vol. 4 (4), pp. 889-940, 1990.

[59] Bhatnagar, A., Choi, Y., Yoon, Y., Jeon, B. , "Bromate removal from water by granular ferric hydroxide (GFH)," *Journal of Hazardous Materials,* vol. 170, no. 1, pp. 134-140, 2009.

[60] Liu, T., Cui, F. Liu, D., Zhao, Z., "Removal of bromate from water using modified activated carbon," *Water Science & Techonology,* vol. 12 (3), pp. 398-405, 2012.

[61] Day, J., Vonderheide, A., Caruso, J., "Automated Real-Time Determination of Bromate in Drinking Water Using LC-ICP-MS and EPA Method 321.8," *Journal of Power Sources,* vol. 2, pp. 318-325, 2006.

[62] Hatzistavros, V., Koulouridakis,E., Aretaki, I., "Bromate determination in water after membrane complexation and total reflection X-ray fluorescence analysis," *Analytical Chemistry,* vol. 79, pp. 2827-2832, 2007.

[63] Cordeiro, F., Schmitz, F., Emteborg, H., "Determination of bromate in drinking water," JRC European Comission, 2010.

[64] Kang, D., Yu, X., Tong, S. Ge, M., "Performance and mechanism of Mg/Fe layered doible hydroxide for flouride and arsenate removal from aqueous solution," *Chemical Engineering Journal,* vol. 228, pp. 731-740, 2013.

[65] Snyder, S., Vanderford, B., Rexing, D., "Trace analysis of bromate, chlorate, iodate and perchlorate in natural and bottled waters," *Environmental Science and Technology,* vol. 39, pp. 4586-4593, 2005.

[66] Norma Oficial Mexicana, "NOM-147-SEMARNAT/SSA1-2004," Diario Oficial de la Federación, 2007.

[67] He, J., Wei, M., Li, B., Kang, Y., Evans, D., "Preparation of layered double hydroxides," *Structure and Bonding,* vol. 119, pp. 89-119, 2006.

[68] Madden, J., Avdalovic, N., Haddad, P., "Prediction od retentions times for anions in linear gradient elution ion chromatography with hydroxides eluents using artificial neural networks," *Journal of Chromatography A,* vol. 910, no. 1, pp. 173-179, 2001.

[69] Lv, L., He, J., Wei, M., Evans D., Duan, X., "Uptake of chloride ion from aqueous solution by calcined layered double hydroxides: Equilibrium and kinetic studies," *Water Research,* vol. 40, pp. 735-743, 2006.

[70] Heilweil, E.J., Casassa, M.P., Cavanagh, R.R., "Picosecond vibrational energy transfer studies of surface adsorbates," *Annual Review of Physical Chemistry,* vol. 40, pp. 143-171, 1989.

[71] Jobbágy, M., Síntesis, caracterización, y propiedades de hidróxidos dobles laminares, Buenos Aires: Facultad de Ciencias Exactas y Naturales, Universidad de Buenos Aires, 2003.